Response of osteoblasts and osteoclasts to gravity : analysis by goldfish scales as a model of bone

著者	山本 樹
著者別表示	YAMAMOTO Tatsuki
journal or publication title	博士論文本文Full
学位授与番号	13301甲第5596号
学位名	博士（理学）
学位授与年月日	2022-09-26
URL	http://hdl.handle.net/2297/00068860

Creative Commons : 表示 - 非営利 - 改変禁止
http://creativecommons.org/licenses/by-nc-nd/3.0/deed.ja

博　士　論　文

Response of osteoblasts and osteoclasts to gravity：analysis by goldfish scales as a model of bone

重力に対する骨芽細胞及び破骨細胞の応答：キンギョのウロコを骨モデルとした解析

金沢大学大学院自然科学研究科

自然システム学専攻

学籍番号　1924062012

氏　　名　山本　樹

主任指導教員名　鈴木信雄

提出年月　2022 年 10 月

CONTENTS

I . General Introduction

It is well known that astronauts experience decreased bone mass after long space flights. For example, it has been reported that bone mass in the hip and spine decrease by about 1% per month under microgravity conditions during space flight (Schneider *et al.*, 1995). Under microgravity conditions, therefore, astronauts suffer from bone disease caused by a decline in bone mass. This disease is one of the main problems during space flight. Furthermore, several factors such as some hormones and bioactive substances in addition to gravity stimuli are associated with bone disease (Suzuki *et al.*, 2008a; Eimori *et al.*, 2016). There are many points needing clarification about the detailed mechanisms of bone disease under microgravity due to the lack of a suitable bone model system to analyze the responses of gravity unloading.

Bone is an active connective tissue composed of three types of cells: osteoblasts, osteoclasts, and osteocytes (Civitelli, 2008; Schaffler and Kennedy, 2012; Chen *et al.*, 2018). Osteoblasts are bone-forming cells that secrete bone matrix to form hard bone, and osteoclasts are bone-absorbing cells that elute the bone matrix by several enzymic actions. Osteocytes are derived from fully differentiated and mature osteoblasts and are buried in the bone matrix secreted by osteoblasts (Al-Bari and Al Mamun, 2020). Osteocytes act as a leading commander of bone remodeling, sensing and integrating mechanical and chemical signals from the environment to regulate bone formation and bone resorption (Schaffler *et al.*, 2014). These bone cells act to maintain bone homeostasis resulting from the regulation of blood calcium ion levels (Al-Bari and Al Mamun, 2020). Therefore,

it is quite important to keep well-balanced bone homeostasis. However, the breakdown of bone homeostasis causes osteoporosis due to the predominance of bone resorption over bone formation, and, conversely, the predominance of bone formation such as calcification causes bone diseases such as osteopetrosis (Brockstedt *et al.*, 1996; Dalbeth *et al.*, 2010; Lerner, 2006).

Space experiments using rats and simulated unloading caused by the suspension of the hind limbs with rats have been conducted (Vico *et al.*, 1993; Wronski and Morey, 1982). However, the results are inconsistent, and many points remain unclear (Chatziravdeli *et al.*, 2019). Under *in vivo* conditions, bone homeostasis is affected by some bioactive substances (e.g., growth factors, cytokines, chemokines) and sexual hormones (estrogen) (Al-Bari and Al Mamun, 2020). Therefore, an *in vitro* culture system under coexisting conditions with osteoclasts, osteoblasts, and bone matrix is desired in order to accurately analyze the bone metabolic response to physical stimuli such as hypergravity and microgravity. However, unlike osteoblasts with established cell lines, osteoclasts need to be induced to a multinucleated active form by cell fusion and are not easy to culture (Sambandam *et al.*, 2010; Saxena *et al.*, 2011). It has been elucidated that the interaction between the osteoclast differentiation factor (receptor activator NF-κB ligand: RANKL) expressed on the cell membrane of osteoblasts and the receptor for RANK expressed on the cell membrane of precursor osteoclasts is important for the differentiation of osteoclasts (Teitelbaum, 2000). Therefore, a co-culture of osteoblasts and osteoclasts is necessary for investigating bone

metabolism.

On the other hand, teleost fish have a unique hard tissue, fish scale that consists of osteoclasts, osteoblasts, and calcified bone matrix including a fibrillary layer (a thick, partially calcified layer) and a bony layer (a thin, well-calcified external layer) (Bereiter-Hahn and Zylberberg, 1993; Suzuki *et al.*, 2000; Yoshikubo *et al.*, 2005; Suzuki *et al.*, 2007; Ohira *et al.*, 2007; Suzuki *et al.*, 2008a). The morphological features of fish scales are very similar to those of mammalian membrane bone (Yoshikubo *et al.*, 2005). Fish scales as a bone model have been shown to respond sensitively to bioactive substances and physical stimuli including hypergravity and microgravity (Suzuki *et al.*, 2008a; Suzuki *et al.*, 2008b; Suzuki *et al.*, 2016; Ikegame *et al.*, 2019). Furthermore, fish scales have a characteristic feature—regeneration after the removal of ontogenic scales—and the regenerating scales have higher cell activity and higher responsiveness to hormones than do normal scales (Yoshikubo *et al.*, 2005). In my study, in order to validate goldfish scales as a bone model for the analysis of gravity stimuli, I performed following three experiments.

First, the localization of RANKL-producing cells in the regenerating scales of goldfish was examined. RANKL-induced osteoclast differentiation and the subsequent enhancement of bone resorption activity is regulated by the master regulator of osteoclast formation (nuclear factor of activated T-cell c1: NFATc1) (Smith, 2020). It has been reported that microgravity exposure enhances bone resorption activity and increases the mRNA expression of RANKL of the

regenerating scales (Ikegame *et al.*, 2019). However, the localization of RANKL-expressing cells in the regenerating scales of teleost fish was still unknown. Therefore, the localization of RANKL-positive cells in the regenerating scales of goldfish was examined immunohistochemically. Furthermore, I investigated the induction of signal transduction pathways for osteoclast formation by the addition of exogenous RANKL.

Next, the localization of osteocyte-like cells in the regenerating scales of goldfish was investigated. SCLEROSTIN, a protein encoded by the *Sost* gene, is expressed mainly in osteocytes in mammalian bone (Collette *et al.*, 2013). SCLEROSTIN, a negative regulator of bone formation, acts as an inhibitor of the *Wnt/β*-catenin signaling pathway that positively regulates bone formation. SCLEROSTIN produced by osteocytes is known to be important in responding to physical stimuli (Pajevic *et al.*, 2013; Delgado-Calle *et al.*, 2017; Hinton *et al.*, 2018). However, the localization of SCLEROSTIN-positive cells in the scales of teleost fish was unknown. In my study, the localization of SCLEROSTIN in the regenerating scales of goldfish was investigated at the mRNA and protein expression levels. In addition, the osteocyte-like cells were observed electron microscopically. Next, I evaluated the effect of microgravity by space flight on the mRNA expression of *Sost* in the regenerating scales of goldfish.

Finally, the influence of bone metabolism in response to both hypergravity and microgravity was examined using the regenerating scales of goldfish. In mammalian bone, the mechanisms of converting physical stimuli into biological

responses (called mechanotransduction) remain unknown due to the lack of an appropriate *in vitro* model system (Makihira *et al.*, 2008; Smith, 2020). In addition, there is a lack of agreement regarding the responsiveness of osteoclasts in the *in vitro* cell culture studies of simulated microgravity on the ground and in space experiments (Makihira *et al.*, 2008; Chatziravdeli *et al.*, 2019; Smith, 2020). Osteocytes are known to be the major sensor of mechanical loading in mammalian bone (Tatsumi *et al.*, 2007; Lin *et al.*, 2009; Schaffler and Kennedy, 2012; Alford *et al.*, 2015; Smith, 2020). Therefore, the scales of teleost fish, in which osteocyte-like cells coexist on the bone matrix, in addition to osteoblasts and osteoclasts were used to evaluate the mechanical stimulation. A simulated microgravity environment was made using a three-dimensional (3D) clinostat, and a comparison between the simulated microgravity environment and the space flight (microgravity) environment was carried out. In my study, the response of osteoblasts and osteoclasts to the physical stimuli of hypergravity and microgravity was analyzed simultaneously for the first time in molecular biology and morphology using the regenerating scales of goldfish.

The present study provides evidence to prove that teleost scales are an excellent model system for analyzing the effects of physical stimuli on bone metabolism.

Ⅱ. Detection of RANKL-expressing cells and response of exogenous RANKL to osteoclasts in regenerating scales of goldfish

Introduction

The receptor activator of nuclear factor-κB (RANK) expressed in osteoclasts and the RANK ligand (RANKL) is important for bone cell interaction (Nagy and Penninger, 2015; Ono and Nakashima, 2018). The binding of RANK to RANKL induces osteoclastic activation (Nagy and Penninger, 2015; Ono and Nakashima, 2018); thus, RANKL has an important function in osteoclastogenesis and causes bone resorption (Teitelbaum, 2000; Kondo *et al.*, 2001). In addition, the nuclear factor of activated T cells cytoplasmic 1 (NFATc1), which is the master regulator of osteoclastogenesis, is activated by RANK/RANKL signaling and induces the expression of osteoclastogenic genes (Takayanagi *et al.*, 2002; Asagiri *et al.*, 2005; Yamashita *et al.*, 2007). The activation of NFATc1 enhances the expression of various molecules involved in the differentiation of osteoclast precursor cells, preosteoclast multinucleation, osteoclast bone resorption activity, or communication between osteoblasts and osteoclasts (Fig. 1) (Takayanagi *et al.*, 2002; Asagiri *et al.*, 2005; Zhao *et al.*, 2006; Yang *et al.*, 2008; Miyauchi *et al.*, 2010; Zhang *et al.*, 2014).

Teleost fish have scales containing osteoblasts, osteoclasts, and a calcified bone matrix that has two layers: a thin, fully calcified outer layer, and an osseous layer, which is a thick, weakly calcified layer (Bereiter-Hahn and Zylberberg, 1993; Yoshikubo *et al.*, 2005; Suzuki *et al.*, 2007; Ohira *et al.*, 2007; Suzuki *et al.*, 2008a). Therefore, in previous studies, fish scales were used as a bone model to evaluate the effects of several physical stimuli, including hypergravity and microgravity stimuli, and to examine the influence of the bioactive substances (Suzuki *et al.*, 2008a; Suzuki *et al.*, 2008b; Suzuki *et al.*, 2016; Ikegame *et al.*, 2019). Teleost fish scales regenerate after being removed (Suzuki *et al.*, 2009; Kakikawa *et al.*, 2012). Previous studies have shown that the bone formation in regenerating scale is very similar to that of the calvarial bone (Yoshikubo *et al.*, 2005; Thamamongood *et al.*, 2012). These regenerating scales were used to demonstrate that microgravity stimulates osteoclast multinucleation and resorption activity (Ikegame *et al.*, 2019). The promotion of osteoclast multinucleation and resorption activity in the regenerating scales was quite similar to the *in vivo* conditions of mammalian bone in space flight (Tamma *et al.*, 2009; Gerbaix *et al.*, 2017). Microgravity induces osteoclastic activation by increasing *Rankl* mRNA expression levels in the regenerating scales (Ikegame *et al.*, 2019). However, the location of RANKL-

producing cells in the regenerating scale remains unknown. Therefore, I prepared antiserum against goldfish RANKL and found RANKL-producing cells in the regenerating scales of goldfish. In addition, in order to investigate RANKL-signaling molecules containing NFATc1, I investigated the effect of exogenous RANKL on osteoclast formation in the regenerating scales of goldfish.

Materials and Methods

Animals

All goldfish (*Carassius auratus*) (20–30 g, male) used in this experiment were purchased from a commercial source (Higashikawa Fish Farm, Yamatokoriyama, Japan). All experimental procedures were carried out according to the Guide for the Care and Use of Laboratory Animals of Kanazawa University.

Immunohistochemical analysis of RANKL in the regenerating scales of goldfish

The goldfish RANKL antiserum was synthesized by Medical and Biological Laboratories Co., Ltd. (Nagoya, Japan). Rabbits were injected with two RANKL peptide sequences (YLRNHIDMEEAPARAPHC and CLASPQQSPNEEMHSETL, GenBank ID: AB894120) of *Carassius auratus* bound to keyhole limpet hemocyanin to obtain the antiserum.

Normally developed scales were removed from goldfish anesthetized with ethyl 3-aminobenzoate methanesulfonic acid salt (Ms-222, Sigma-Aldrich) to regenerate the scales. Two weeks later, the goldfish were anesthetized, and the

regenerated scales were removed and fixed with a 4% paraformaldehyde solution in phosphate-buffered saline (PBS). After rinsing with PBS, the scales were incubated for 1 hour at room temperature in a solution containing 0.1% Tween 20, 0.3% glycine, 10% normal goat serum, and 1% bovine serum albumin (BSA). The scales were then incubated overnight at 4°C with anti-RANKL serum (2,000x), rinsed with PBS, and incubated with Alexa Fluor 488-labeled anti-rabbit IgG (1,000x; A11034, Molecular Probes) for 1 hour at room temperature. After washing again with PBS, the nuclei were stained with 4', 6-diamidino-2-phenylindole (DAPI). As a negative control, normal rabbit serum was used for overnight immunostaining at a temperature of 4°C. Samples were evaluated using a fluorescence microscope (BX51, Olympus).

Effect of exogenous RANKL on osteoclastogenesis in goldfish scales regenerating in culture

Goldfish were anesthetized with Ms-222, and the scales were collected and cut in half. Next, half of each piece was put into a 24-well microplate with 1 mL of Leibovitz's L-15 medium (Thermo Fisher Scientific) supplemented with mouse RANKL (150 ng/mL) (R&D Systems), antibiotics, and 2% BSA. The other half of

the scale was placed as a control in another well of a microplate containing RANKL-free medium. These scales were incubated in L-15 medium at 15℃ for 3 and 6 hours. After incubation, the scales were frozen at -85℃ until the next mRNA analysis by quantitative real-time PCR. The mRNA expressions of the control and experimental scales from the same fish were compared.

Quantitative real-time PCR analysis

Total RNA was isolated from goldfish scales using a total RNA isolation kit for fibrous tissue (RNeasy Fibrous Tissue Mini-Kit, Qiagen), followed by complementary DNA synthesis. PCR amplification was analyzed using a real-time PCR apparatus (Mx3000pTM, Stratagene) with specific primers for *B lymphocyte-induced maturation protein-1* (*Blimp1*), *cathepsin K* (*Ctsk*), *dendritic cell-specific transmembrane protein* (*Dc-stamp*), *elongation factor-1 alpha* (*Ef-1α*), *ephrinB2*, *Nfatc1*, and *osteoclast stimulatory transmembrane protein* (*Oc-stamp*) (Table 1). PCR conditions have been previously described (Suzuki *et al.*, 2011; Sato *et al.*, 2017; Ikegame *et al.*, 2019).

Statistical analysis

Data are presented as the means ± the standard error of the mean (SEM). Statistical significance was assessed using the paired Student's *t*-test. The selected significance level was $p < 0.05$.

Results

Immunohistochemical analysis of RANKL in regenerating scales of goldfish

Antiserum against the goldfish RANKL was prepared in rabbits to determine the localization of RANKL-expressing cells. The presence of positive RANKL immunostaining was shown by immunohistochemical analysis in some mononuclear cells located in the grooves of goldfish scales regenerating for 14 days (Fig. 2).

Effects of the addition of exogenous RANKL on osteoclastogenesis in cultured regenerating scales of goldfish

In order to evaluate the effects of RANKL on the osteoclastogenesis of regenerating scales, mouse RANKL was added to the medium, and gene expression was assessed. The mRNA expression of the transcription factor, *Nfatc1*, was significantly upregulated by RANKL treatment for 3 hours (Fig. 3A). After 6 hours of incubation with RANKL, the mRNA expression of the osteoclast function gene *Ctsk* was significantly upregulated (Fig. 3B). In addition, the mRNA levels

of factors involved in osteoclast multinucleation, such as *Oc-stamp* and *Dc-stamp*, were elevated after treatment with RANKL (Fig. 4). Significant differences in the mRNA levels of *Dc-stamp* and *Oc-stamp* were observed between the control and experimental groups after 3 hours of incubation with RANKL (Fig. 4). The 6-hour incubation with RANKL resulted in a statistically significant difference in *Oc-stamp* mRNA expression levels between the treatment and control groups (Fig. 4). After 3 hours of incubation with RANKL, the mRNA expression of *Blimp1* significantly increased in the treated group as compared to the control levels (Fig. 5). The mRNA expression of *EphrinB2* also tended to increase with 3 hours of treatment of scales with RANKL as compared with untreated controls ($p = 0.07$, Fig. 5).

Discussion

In this study, RANKL-producing cells were detected in the grooves of regenerating goldfish scales (Fig. 2). Most osteoclasts were also present in the grooves of regenerating scales. Previous studies have shown that under microgravity for spaceflight, there are multinucleated cells in the grooves, and remarkable bone resorption is induced after 86 hours of incubation under microgravity (Ikegame *et al.*, 2019). These findings show that RANKL-producing cells communicate with osteoclasts and induce osteoclastogenesis in the grooves of regenerating scales. One cause of this osteoclastic activation is the increased expression of RANKL, as *Rankl* mRNA expression actually increased under microgravity (Ikegame *et al.*, 2019). Based on these findings, I aimed to investigate the effect of extrinsic RANKL on osteoclastogenesis in cultured and regenerating scales of goldfish.

It was found that recombinant mouse RANKL effectively promotes osteoclastic activation of goldfish osteoclasts (Figs. 3–5). The mRNA expression of transcription factor *Nfatc1*, the master regulator of osteoclast formation, was

significantly increased after 3 hours of incubation with RANKL, as compared with the level of untreated control cells. In addition, the mRNA expression of *Ctsk*, the osteoclastic functional gene, was markedly upregulated after 6 hours of incubation with RANKL. After incubating with RANKL for 3 and 6 hours, the mRNA expressions of *Dc-stamp* and *Oc-stamp*, which are essential for osteoclast multinucleation (Yang *et al.*, 2008; Zhang *et al.*, 2014), were also upregulated (Fig. 4). In addition, the mRNA expression of *Blimp1*, a factor involved in osteoclast differentiation (Miyauchi *et al.*, 2010), was increased by treatment with RANKL (Fig. 5). RANKL signaling was induced by the addition of extrinsic RANKL in both fish scale osteoclasts and mammalian bone. Also, the mRNA expression of *EphrinB2* was elevated (Fig. 5). After bone resorption, coupling and bone remodeling are induced by EPHRINB2 (Zhao *et al.*, 2006; Matsuo and Otaki, 2012). Therefore, it is suggested that RANKL treatment may promote remodeling in scales, as well as in mammalian bone. Future plans include determining the detailed RANKL signaling pathways using regenerating goldfish scales.

Teleost fish scales are simple calcified tissues that coexist with osteoblasts, osteoclasts, and bone matrix. Because fish scales have bone-like characteristics, they are sensitive to microgravity (Ikegame *et al.*, 2019) and hyperloading, such

as centrifugation and vibration (Suzuki *et al.*, 2007; Suzuki *et al.*, 2008b; Suzuki *et al.*, 2009; Kakikawa *et al.*, 2012). Additionally, it was reported that fish scales respond to low-intensity pulsed ultrasound (LIPUS) (Hanmoto *et al.*, 2017). After 6 hours of incubation with LIPUS treatment, *Rankl* mRNA expression was significantly increased. Due to elevated expression levels of *Rankl* mRNA, transcriptional regulator expression was significantly increased after 6 hours of ultrasound treatment with LIPUS, and mRNA expression of functional genes was significantly elevated after 12 hours of incubation with LIPUS. Bone matrix plays an important role in the response to physical stimuli (Owan *et al.*, 1997; Hoffler *et al.*, 2006; Watabe *et al.*, 2011). Because fish scales are made up of calcified tissue that coexists with osteoblasts, osteoclasts, and bone substrates, RANKL expression may be sensitive to LIPUS stimuli.

In addition to the above physical stresses, some calcium hormones work in osteoblasts and osteoclasts. Parathyroid hormone (PTH), a hypercalcemia hormone, acts on the osteoblasts of goldfish scales to activate osteoclasts *via* the RANK/RANKL pathway, in a manner similar to that of mammalian osteoblasts and osteoclasts (Suzuki *et al.*, 2011). In goldfish, prostaglandin E_2 (PGE_2) acts on osteoblasts and increases osteoclast activity in goldfish scales via the

RANK/RANKL pathway (Omori *et al.*, 2012). Increased *Rank1* mRNA expression by PGE_2 treatment induces hypercalcemia in goldfish.

Based on these previous studies and the results obtained in this study, RANKL has an important function in the metabolism of fish bone as well as that of mammals, and I conclude that it is a suitable model for evaluating some physical stimuli or bioactive substances of fish scales. Hereafter, I plan to investigate the mechanism of osteoclast activation by microgravity *via* RANKL in more detail.

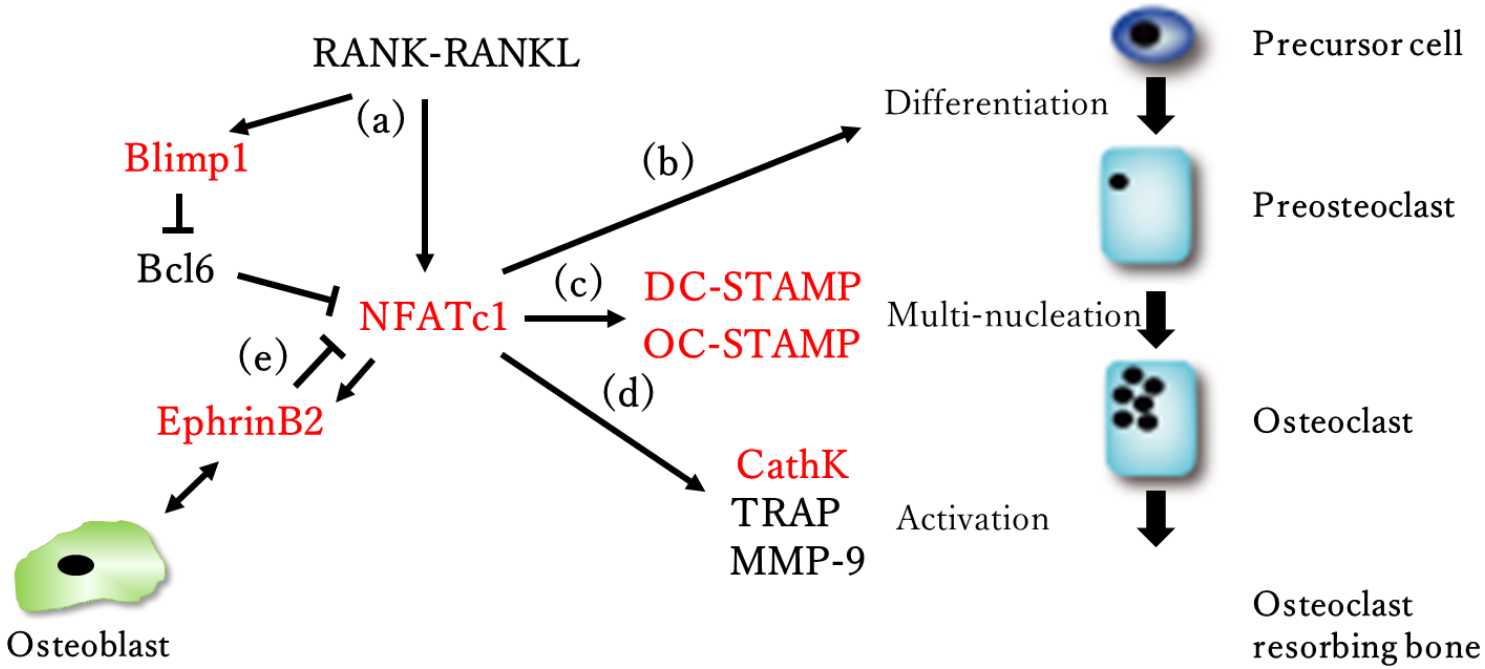

Fig. 1. RANK/RANKL-dependent signaling pathway regulating osteoclastogenesis. (a) The RANK/RANKL signaling pathway induces the NFATc1 expression of and/or by inducing BLIMP1 to inhibit the BCL6-dependent suppression of *Nfatc1* transcription. (b) Induction of NFATc1 promotes the differentiation of precursor cells into preosteoclasts. (c) Next, NFATc1 stimulates the transcription of DC-STAMP and OC-STAMP, whose protein products are involved in the multinucleation of preosteoclasts. (d) NFATc1 subsequently increases the expression of CTSK, TRAP, and MMP9, all of which are factors required for the bone resorption activity of osteoclasts. (e) NFATc1 promotes osteogenic differentiation via EPHRINB2-mediated signal from osteoclasts to osteoblasts, while the signals inhibit the expression of NFATc1, which suppresses osteoclast differentiation. Molecules analyzed in the current study are shown in red.

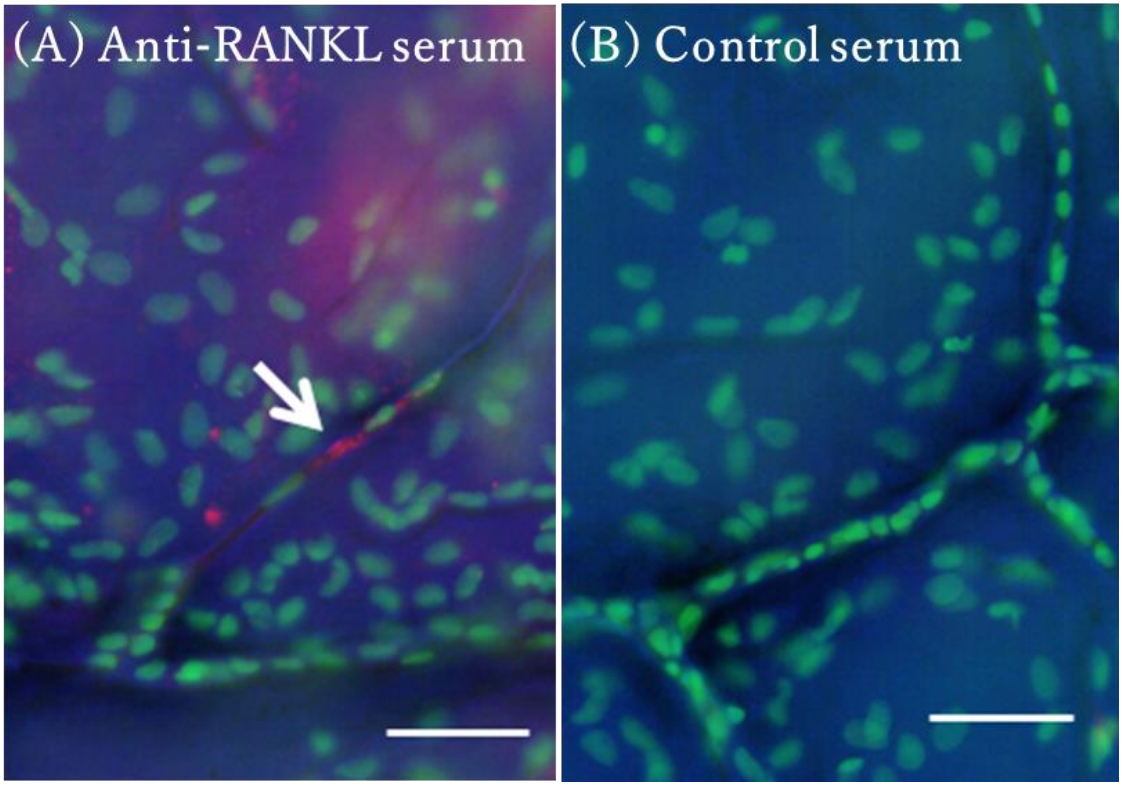

Fig. 2. Immunohistochemical detection of RANKL in regenerating scales after 14 days of regeneration. RANKL immunostaining (red, indicated by the arrow) overexposed with DAPI staining (green) (A). As a negative control, immunostaining was performed overnight at 4℃ using normal rabbit serum and overexposed with DAPI staining (green) (B). Scale bar, 50 μm.

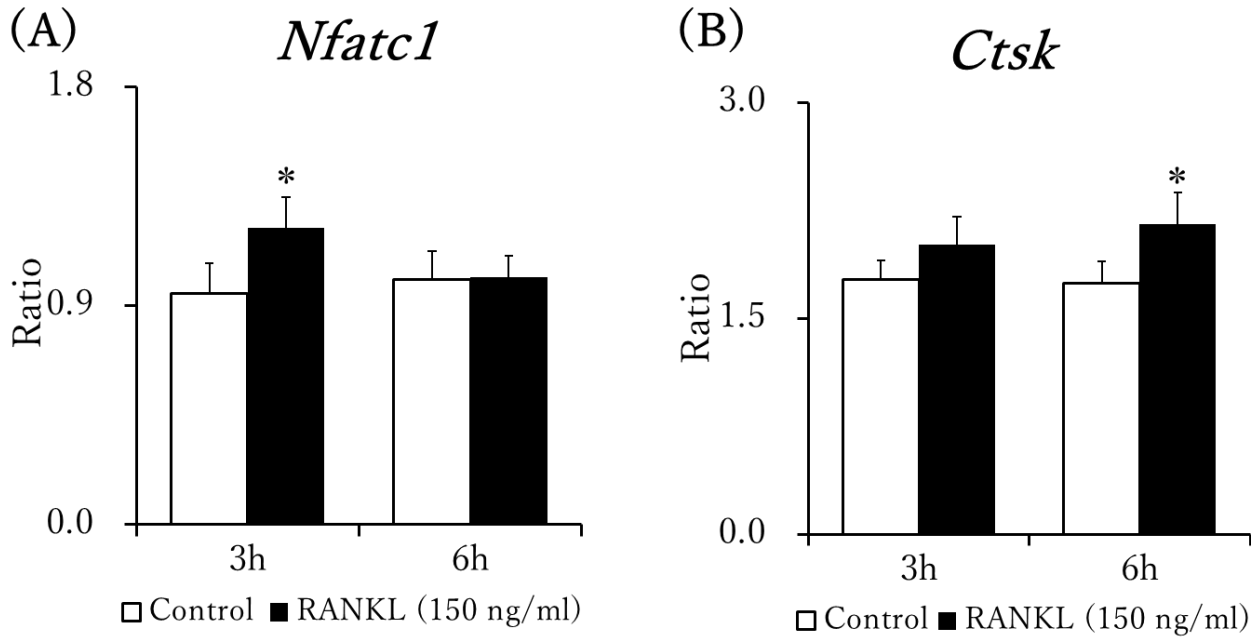

Fig. 3. Effects of exogenous RANKL on mRNA expression levels of *Nfatc1* (A) and *Ctsk* (B) in the cultured regenerating scales of goldfish after 3 and 6 h of incubation. Data represent the mean ± S.E.M. ($n = 11$). * indicates a p-value of less than 0.05 versus the control using a paired t-test.

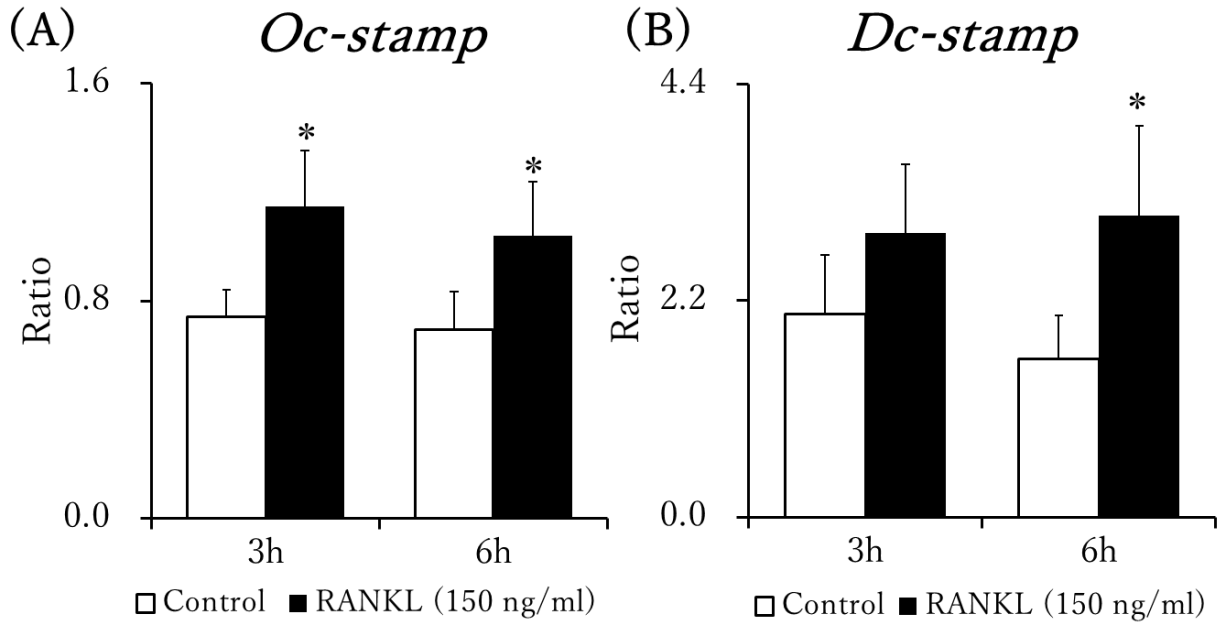

Fig. 4. Effects of exogenous RANKL on mRNA expression of *Oc-stamp* (A) and *Dc-stamp (B) in cultured regenerating scales of goldfish after 3 and 6 h of incubation.* Data represent the mean ± S.E.M. ($n = 11$). * indicates a p-value of less than 0.05 versus the control using a paired t-test.

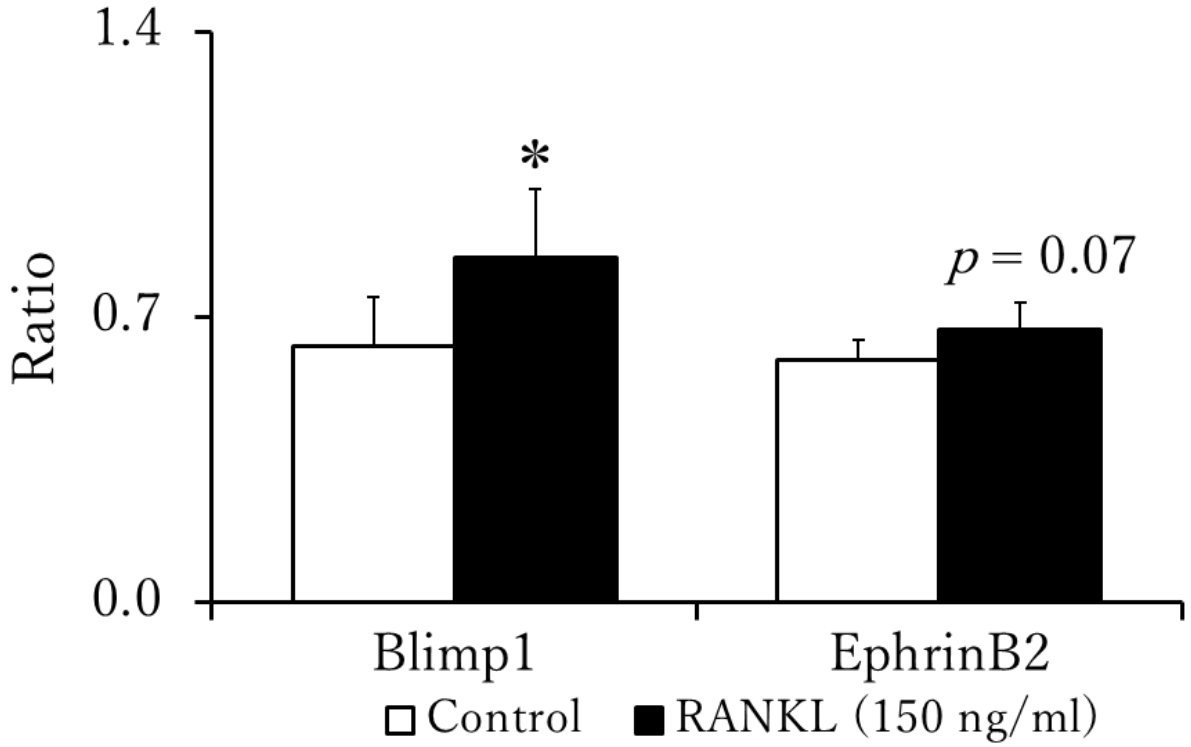

Fig. 5. Effects of exogenous RANKL on mRNA expression of *Blimp1* and *Ephrinb2* in cultured regenerating scales of goldfish at 3 hours of incubation. Data represent the mean ± S.E.M. (n = 6). * indicates a p-value of less than 0.05 versus the control using a paired t-test.

Table 1. Primer sequences used for quantitative RT-PCR

Target gene	Forward sequence (5' → 3')	Reverse sequence (5' → 3')
Nfatc1	CTGTCGTGCGTTTTGGGAAAG	GATGCTGGTGTTTTGGCTGTAACC
Ctsk	TGGGAGGGCTGGAAACTCAC	CATGAGCCGCATGAACCTTG
Oc-stamp	TGTGGTGCTGTTTGTCCTACC	CAACCGTCCCTTCACTTCTG
Dc-stamp	TTCGCTGTTTTGGAGCCTTG	TGCTTTCCCACCCATTTTAGC
Blimp1	ATGGAAGGGTTTGACGTGGAGAGC	ATGTAGATAATGCAGGTGCTGGGGG
EphrinB2	AGAAACGGACCAAAGGAAGG	CACAATCGGAGCCTGAAAGA
Ef1a	ATTGTTGCTGGTGGTGTTGG	GGCACTGACTTCCTTGGTGA

Ⅲ. Sclerostin expression in regenerating goldfish scales and its change under microgravity during space flight

Introduction

Osteoblasts and osteoclasts are two major types of cells that regulate bone metabolism. Osteoblasts are involved in the formation of new bone, and osteoclasts are involved in the resorption of aged bone (Henry and Bordoni, 2020). Sclerostin, a protein encoded by the *Sost* gene, works as an important negative regulator of bone formation. *Sost* mutations cause several bone diseases characterized by high bone mass, such as sclerosteosis and Van Buchem disease (Balemans *et al.*, 2001; Brunkow *et al.*, 2001; Balemans *et al.*, 2002; Staehling-Hampton *et al.*, 2002). In bone, SOST is predominantly expressed in osteocytes; however, osteoblasts and osteoclasts have been found to have very low SOST expression levels (Collette *et al.*, 2013). At the molecular level, the binding of sclerostin to the LRP5/6 receptor inhibited the Wnt/β-catenin signaling pathway and reduced bone formation (Poole *et al.*, 2005; Li *et al.*, 2005; Ellies *et al.*, 2006). Both *Sost*$^{-/-}$ and osteocyte-depleted mice have been reported to exhibit resistance to bone loss induced by hindlimb unloading *via* tail suspension (Tatsumi *et al.*, 2007; Lin *et al.*, 2009). These previous studies provide evidence that osteocyte-

produced sclerostin plays an important role in responding to mechanical stimuli (Pajevic *et al.*, 2013; Delgado-Calle *et al.*, 2017; Hinton *et al.*, 2018).

In mammalian bone, osteoblastic cells regulate the differentiation and activation of osteoclasts (Kondo *et al.*, 2001; Kearns *et al.*, 2008; Lacey *et al.*, 2012). Several stromal cells, such as osteoblasts and bone marrow cells, expressed RANKL. RANKL binds to RANK (receptor of RANKL) on osteoclasts and enhances osteoclast differentiation and activation (Kearns *et al.*, 2008; Kondo *et al.*, 2001). The effect of RANKL on osteoclasts is inhibited by the decoy receptor osteoprotegerin (OPG) produced by stromal cells (Kearns *et al.*, 2008; Kondo *et al.*, 2001). Mammalian sclerostin suppresses OPG production and promotes osteoclastogenesis by inhibiting Wnt signaling in stromal cells (Kubota *et al.*, 2009; Silva and Branco, 2011; Pajevic *et al.*, 2013; Delgado-Calle *et al.*, 2017).

Several groups have reported that fish scales are morphologically and functionally similar to mammalian bones in some respects. Fish scales contain osteoblasts, osteoclasts, and a mineralized matrix (osseous layer on the epithelial side) with a collagen-rich matrix (fibrous layer on the dermal side) (Bereiter-Hahn and Zylberberg, 1993; Azuma *et al.*, 2007; Ohira *et al.*, 2007; Suzuki *et al.*, 2007; Suzuki *et al.*, 2008b; de Vrieze *et al.*, 2014). Fish scales have been

established as a useful experimental system for *in vitro* analysis of mammalian bone metabolism (Suzuki *et al.*, 2000; Suzuki and Hattori, 2002). In this system, the expression of genes involved in bone metabolism and the activity of osteoblasts or osteoclasts have been shown to be highly sensitive to various mechanical stimuli, including static hypergravity due to centrifugation (Suzuki *et al.*, 2008b), dynamic hypergravity due to vibration (Suzuki *et al.*, 2007; Suzuki *et al.*, 2009), ultrasound (Kitamura *et al.*, 2010; Suzuki *et al.*, 2016; Hanmoto *et al.*, 2017), and microgravity in outer space (Ikegame *et al.*, 2019). These reports provide evidence that fish scale is an appropriate experimental model for analyzing the response of bone metabolism to mechanical stimuli.

The current study revealed for the first time that sclerostin is produced in goldfish scales at the mRNA and protein levels. I also found evidence that osteoblast-like cells in the calcification matrix and osteoblasts in scales are responsible for sclerostin production. Finally, I discovered that outer space microgravity increases the expression of *Sost* in scales, which may be the mechanism of osteoclast activation.

Materials and Methods

Animals

One male and one female goldfish (*Carassius auratus*) were purchased from Higashikawa Fish Farm (Yamatokoriyama, Japan). Artificial insemination was performed at the Tokyo University of Marine Science and Technology, and fertilized eggs were obtained. The eggs were grown to adult fish with body lengths of 12–15 cm. After that, adult fish were transferred to the Tokyo Medical and Dental University and Kanazawa University and adopted for *in vitro* experiments. The fish were fed a commercial pellet feed for blowfish every morning and kept in fresh water at 26°C until used. All experimental procedures were performed according to the Guide for the Care and Use of Laboratory Animals prepared by the Tokyo Medical and Dental University and Kanazawa University.

Preparation of regenerating goldfish scales

Goldfish were anesthetized with 0.03% Ms-222 (Sigma-Aldrich), and fully grown scales were removed to allow scale regeneration. On the 15th day after

removal, the regenerating scales were removed from the goldfish and used in the experiment.

In situ hybridization

Using digoxigenin (DIG) RNA Labeling Kits (Roche), DIG-labeled sense and antisense single-stranded RNA probes for goldfish *Sost* were prepared according to the manufacturer's instructions. The cDNA sequence used to prepare the probe was a 293 bp fragment (AB970730).

The regenerating scales were fixed with 4% paraformaldehyde (PFA) solution in PBS. After washing with RNAse-free PBS, the scales were applied as whole-mount samples or embedded in Tissue-Tek® optimal cutting temperature compound for the preparation of cryosections. After pretreatment with proteinase K, 0.2 N HCl, and 0.25% acetic anhydride, whole-mount and cryosection samples were then hybridized with the probes at a final concentration of 1 μg/mL in a hybridization solution composed of 50% deionized formamide, 5 × saline-sodium citrate (SSC), 2% blocking reagent, 0.1% N-lauroylsarcosine, 0.02% SDS, and 200 μg/mL tRNA at 55°C overnight. After hybridization, sections were rinsed with 0.1 × SSC and 2 × SSC and then treated with ribonuclease. The signals of

the probe were detected with an anti-DIG antibody bound to alkaline phosphatase in accordance with the manufacturer's protocol (DIG Detection Kit; Boehringer Mannheim). The samples were counterstained with methyl green and examined under a light microscope to visualize the nuclei.

Immunohistochemistry

The rabbit anti-human sclerostin antibody (N-terminal 12–42) (ab63097, Abcam) was used as the primary antibody. Similarly to the method described above, the regenerating scales were fixed in 4% PFA solution in PBS to prepare whole-mount or cryosection samples of the scales. The samples were incubated for 1 hour at room temperature in a blocking solution containing 10% normal goat serum, 1% BSA, 0.3% glycine, and 0.1% Tween-20. Next, they were incubated overnight with primary antibodies (x100) at a temperature of 4℃, washed with PBS, and then incubated with Alexa Fluor® 488-labeled goat anti-rabbit IgG (A11034, Molecular Probes; x 1000) for 1 hour at room temperature. Subsequently, they were rinsed with PBS and then stained with DAPI to visualize the nuclei. To prepare a negative control sample, the procedure outlined above was performed using normal rabbit serum instead of anti-sclerostin as the primary

antibody. Samples were observed using a fluorescence microscope (BX51, Olympus).

Transmission electron microscopy

The regenerating scales were fixed overnight at 4°C with 4% PFA and 4% glutaraldehyde in 0.1 M phosphate buffer. The samples were thoroughly rinsed with 0.1 M phosphate buffer, fixed with 1% osmium tetroxide (Merck KGaA) at 4°C for 1 hour, dehydrated in the specimens, and dehydrated with graded ethanol. After treatment with propylene oxide for 5 minutes, the samples were impregnated with Epon 812 (TAAB Laboratories), and the accelerator DMP-30 was added. The samples were then cured at 60°C for 2 days. Using a diamond knife, ultrathin sections perpendicular to the scale surface were cut. The sections were then stained with aqueous lead citrate. Some samples were decalcified with 5% EDTA for 4 days after fixation and treated as described above. The ultrathin sections obtained from the decalcified samples were stained with 1% tannic acid, aqueous lead citrate, and alcoholic uranyl acetate. All ultrathin sections were observed with a transmission electron microscope (H-7100; Hitachi) at an acceleration voltage of 100 kV.

Space experiment at the International Space Station

Goldfish were anesthetized with 0.03% Ms-222 (neutralized using $NaHCO_3$), and following the procedures for scale removal as shown by Suzuki *et al.* (2009), scales ware removed one by one using sharp forceps. After that, goldfish were maintained at 26℃. On the 12th day after scale removal, the goldfish were bred in water using the anti-infective reagent Green F Gold (Japan Pet Design). The next day, some regenerating scales were collected from each goldfish. Scales with similar cellular activity were selected as previously described (Ikegame *et al.*, 2019). Subsequently, on day 14, the regenerating scales were sampled from goldfish on ice that had been sterilized using fungizone and hypochlorite solutions and immersed in Leibovitz's L-15 medium containing 10% FCS, 100 μg/mL streptomycin, 100 U/mL penicillin, and 200 μg/mL kanamycin. After that, the sterilized scales were packed in a culture chamber (Cell Experiment Small Chamber, Chiyoda Corporation). The culture chambers were kept at temperatures from 2.5 to 4.0℃ and sent via the Space Shuttle Atlantis (STS-132) to the International Space Station (ISS) (Yano, 2011). After arriving at the ISS, they were cultured for 86 hours under microgravity at the Cell Biology Experiment

Facility (CBEF) (Yano, 2011). The CBEF is equipped with a centrifuge for processing samples with a single gravity [artificial microgravity in flight (F-1g)] (Yano *et al.*, 2012). The facility is capable of culturing biological samples in a temperature range of 15℃ to 40℃ (Yano *et al.*, 2012). Differences among the sensors ranged from 0.1℃ to 0.2 ℃ (Yano *et al.*, 2012). During culturing in the CBEF, the culture chambers installed in the microgravity section (F-μg) and 1G section (F-1g) of the CBEF were maintained at 21.9℃ to 22.0℃ in the measurement experiment unit (MEU) (Yano, 2011; Yano *et al.*, 2012). The culture chambers were treated with 1 g of gravity in the 1G section but were maintained in the microgravity section without gravity treatment. After incubation, the culture chambers were removed from the MEU. The medium in the culture chamber was then replaced with RNAlater (Sigma-Aldrich) for gene expression analysis. Scales processed with RNAlater were stored at -96℃ until STS-132 returned to the Kennedy Space Center in Florida.

Real-time quantitative PCR

Total RNA isolation and cDNA synthesis were performed using a kit (Qiagen) and in accordance with the manufacturer's instructions (Ishizu *et al.*, 2018). Each

quantitative real-time (RT)-PCR reaction was performed using a real-time PCR device (Mx3000p, Stratagene). In the PCR reaction, a cDNA template mixed with suitable primers was combined with SYBR Premix Ex Taq (Takara Bio) (Ikegame *et al.*, 2019). The *elongation factor 1α* (*Ef-1α*) gene, a house-keeping gene, was used for normalization. Table 2 shows the PCR primer sequences used in the current study.

Statistics

All results are expressed as the mean ± SEM ($n = 4$). The control scale values were compared to the experimental scale values. The data were evaluated using the Student's *t*-test, and the significance level selected was $p < 0.05$.

Results and Discussion

Detection of cells expressing mRNA of Sost (sclerostin) and its protein in regenerating goldfish scales

Whole-mount *in situ* hybridization (ISH) was performed using the regenerating scales of goldfish to obtain insight into whether fish scale cells express *Sost* mRNA (Figs. 6 and 7). First, I focused on the peripheral area of the scale where ridges and grooves exist (Fig. 6A). ISH signals using the antisense *Sost* probe were detected in a large number of cells located along the ridges and some cells in the grooves (Fig. 6B), but not in the sense *Sost* probe (Fig. 6C). Next, immunohistochemistry (IHC) was performed using the sclerostin antibody. As shown in Fig. 6D, IHC signals were detected primarily in cells located along the medial slope of the ridges and in some cells in the grooves that were not detected by IHC using normal IgG (Fig. 6E). In summary, I found that cells located along the grooves and ridges expressed *Sost* (sclerostin) mRNA and its proteins on regenerating goldfish scales.

Next, I focused on the central area of the scales in which the grooves form a

mesh-like structure (Fig. 7A). Using the antisense *Sost* probe, ISH signals were detected in cells in the grooves (Fig. 7B) but not in the sense *Sost* probe (Fig. 7C). Next, IHC was performed using sclerostin antibodies to evaluate whether cells expressing sclerostin protein were present on the scales. As shown in Fig. 7D, IHC signals were detected in the cells of the grooves, but not with normal IgG (Fig. 7E). Although ISH *Sost* signals were very weak, IHC signals were also detected in cells outside the groove (Fig. 7D). The reason for the different expression profiles between *Sost* mRNA and the sclerostin protein has not been identified. A possible explanation is that *Sost* mRNA and sclerostin protein have different half-lives. Future studies will test this possibility by assessing the time-dependent expression of *Sost* mRNA and sclerostin proteins during goldfish scale regeneration.

It should be noted that some types of cells that regulate bone metabolism, such as osteoclasts and osteoblasts, are reportedly present in the furrows and ridges of regenerating goldfish scales (Yoshikubo *et al.*, 2005; Suzuki *et al.*, 2007; Suzuki *et al.*, 2008a; Yachiguchi *et al.*, 2014; Ikegame *et al.*, 2019; Yamamoto *et al.*, 2020a). Therefore, in addition to whole-mount analysis, cryosections were used to further examine sclerostin-producing cells, as described below.

Cells containing sclerostin are half-embedded cells, osteoblasts, and bone lining cells

ISH was performed using cryosections of the regenerating scales to assess the distribution of cells expressing *Sost* mRNA separately in the bone and fibrous layers of scales (Fig. 8A and 9A). In both the central and peripheral areas of the scale (Fig. 8B and 9C), ISH signals using the antisense *Sost* probe were detected in cells covering the fibrous layer, but not in the cells of the osseous layers, with the exception of a few cells (Fig. 8B) close to the peripheral end of the scale. This result is inconsistent with the above finding that signals were detected in the cells on the osseous layers of grooves and along ridges by whole-mount ISH (Figs. 6 and 7). It is speculated that the intracellular ISH signals in the osseous layer are too weak to be detected in thin cryosections. Signal specificity was confirmed by ISH using the sense *Sost* probe, which did not detect the signals (Figs. 8C and 9D). Next, IHC was performed using sclerostin antibodies (Figs. 8D and 9E), and its specificity was confirmed by IHC using normal IgG (Figs. 8E and 9F). Similarities were found between the distribution of cells containing sclerostin protein and the distribution of cells expressing *Sost* mRNA covering the fibrous layer. In cells of the osseous layer, IHC signals were also detected. The expression

of sclerostin was observed in flat lining cells and half-embedded cells of the mineralization matrix (Figs. 8D and 9E).

Notably, cells with ISH or IHC signals in the fibrous layers were found to have a rounded shape, suggesting that they produced a matrix of scales (Yoshikubo *et al.*, 2005; Suzuki *et al.*, 2007; Suzuki *et al.*, 2008a; Ikegame *et al.*, 2019; Yamamoto *et al.*, 2020a). In addition to round cells, ISH or IHC signals were also detected in flat cells lined up in the osseous layer (Figs. 6D, 7B, 7D, 8D, and 9E) along the surrounding ridges and on the surface of the central mineralized matrix. The shape and condition of the cells correspond to inactive osteoblasts that line cells of bone tissue. Therefore, it is shown that scale osteoblasts expressed *Sost* mRNA.

Furthermore, *Sost*/sclerostin signals were detected in cells half-embedded in a groove or calcified matrix (Fig. 9C and 9E). Based on observation with a transmission electron microscope, two types of half-embedded cells were found in the osseous layer. One type was found at the bottom of the groove in contact with the collagen bundle in the fibrous layer (Fig. 10A). The other type was largely surrounded by the mineralized matrix (Fig. 10B). Therefore, it is speculated that these half-embedded cells are osteocyte-like cells that eventually differentiate from osteoblasts and become implanted in the bone matrix (Sawa *et al.*, 2019).

The basis for this speculation is not just the *Sost*/sclerostin expression and cell localization (half-embedded in the calcification matrix). Osteoclasts have been reported to be present in osseous layers, particularly along grooves, but not in fibrous layers (Ikegame *et al.*, 2019). Additionally, RANKL expression is predominantly found in cells within grooves (Yamamoto *et al.*, 2020a). Therefore, it is speculated that half-embedded osteocyte-like cells in the osseous layers accelerate osteoclast differentiation and activation due to producing RANKL (Yamamoto *et al.*, 2020a), which is similar in mammalian bone (Nakashima *et al.*, 2011).

Increased Sost expression in regenerating goldfish scales under microgravity in outer space

Previous experiments in space on board the ISS have shown that the ratio of osteoclast activity along the grooves and the expression ratio of *Rankl*:*Opg* in goldfish scales increased under microgravity conditions (Ikegame *et al.*, 2019). It has been reported that sclerostin induced RANKL production in osteocytes (Wijenayaka *et al.*, 2011) and suppressed OPG production in osteoblasts and/or osteocytes by interfering with the Wnt signaling pathway to activate osteoclasts

(Kubota *et al.*, 2009; Kobayashi *et al.*, 2016; Delgado-Calle *et al.*, 2017; Figurek *et al.*, 2020). This fact, along with this finding of the existence of sclerostin-producing cells in goldfish scales, indicates that sclerostin may contribute to microgravity-induced osteoclastic activation in goldfish scale. The expression levels of *Sost*, as well as *Dkk1* and *Wif1*, suppressors of the Wnt signaling pathway, in goldfish scales were compared between those kept under microgravity conditions in outer space (F-μg) and those of goldfish scales treated with 1 g gravity in outer space (F-1g). Microgravity was found to increase *Sost* expression, but it did not affect *Dkk1* or *Wif1* (Fig. 11).

Sost/sclerostin expression is known to be upregulated by mechanical unloading, and it has an important function in the mechanical response of bone (Robling *et al.*, 2008; Lin *et al.*, 2009). The results of this research showed for the first time that the expression of *Sost* in fish scales is stimulated by microgravity. In support of the discussions in this study, it was reported that, resulting from 30 days of space flight, *Sost* expression levels in mouse calvaria were significantly higher than those in ground controls (Macaulay *et al.*, 2017). These facts suggest the underlying mechanisms of bone loss, such as osteoporosis in outer space: microgravity increases sclerostin production by promoting the expression of the

Sost gene. The increase of sclerostin induced the over-activation of osteoclasts and then led to a loss of bone mass.

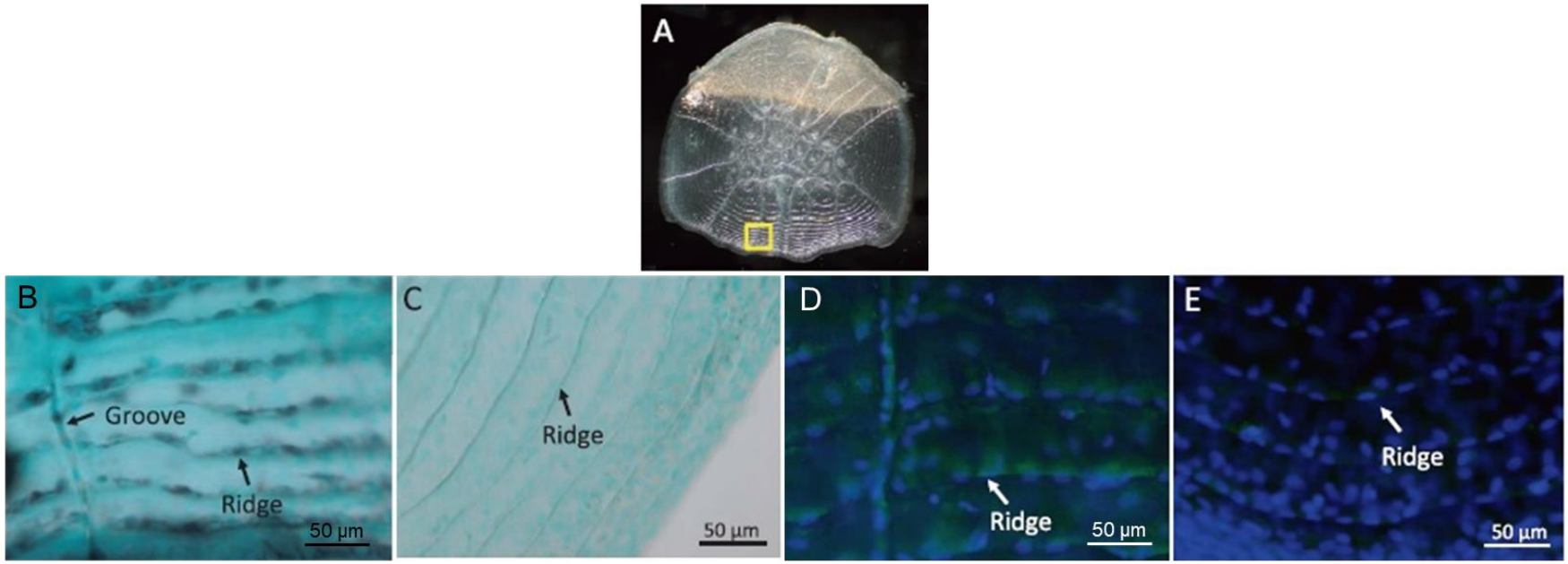

Fig. 6. Whole-mount detection of *Sost*/sclerostin in the peripheral area of the regenerating scales by *in situ* hybridization (ISH) and immunohistochemistry (IHC). A: Binocular view of regenerating scale on day 15. The parts corresponding to the area in the yellow square are magnified and shown in B to E. B: Detection of *Sost* mRNA with an antisense probe by ISH (dark purple). C: Negative control for ISH with *Sost* sense probe. D: Detection of sclerostin with anti-sclerostin antibody by IHC (green color). E: Negative control for IHC with normal rabbit IgG. Arrows indicate grooves or ridges. Nuclei were stained with methyl green in B (light green) and C (light green) and with 4′ , 6-diamidino-2-phenylindole in D (blue) and E (blue). The images were taken from the epithelial side (osseous layer) of scale.

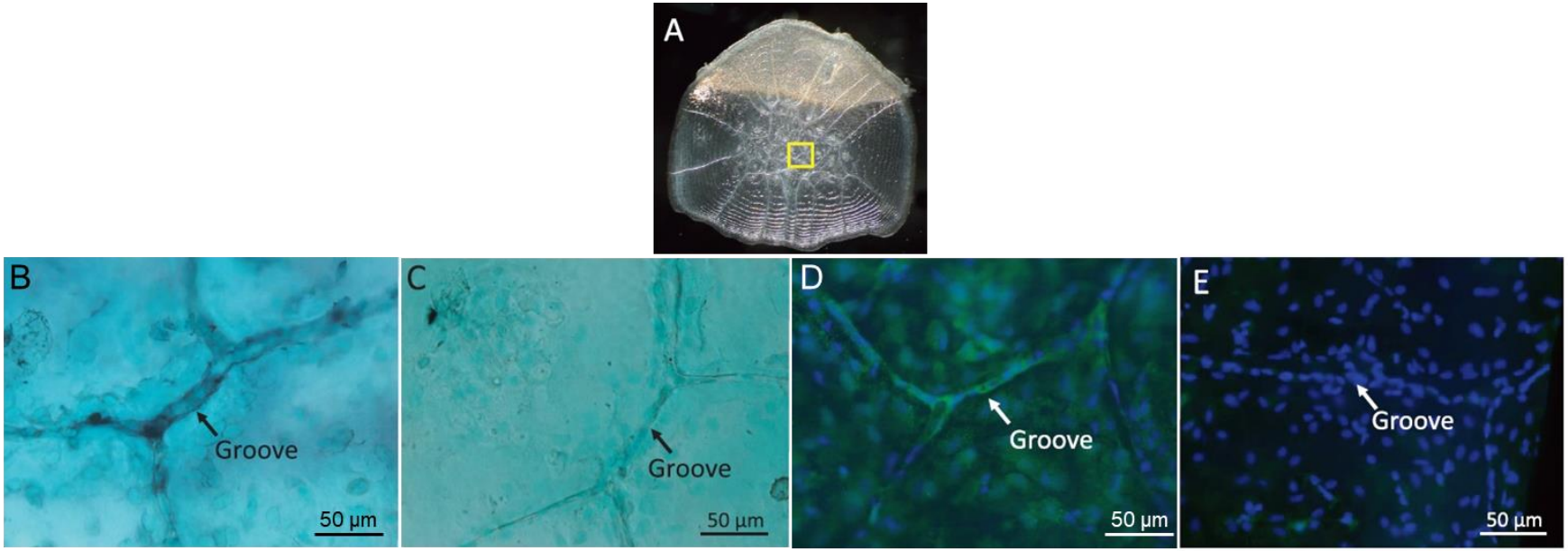

Fig. 7. Whole-mount detection of *Sost*/sclerostin in the central area of the regenerating scales by *in situ* hybridization (ISH) and immunohistochemistry (IHC). A: Binocular view of regenerating scale on day 15. The parts corresponding to the area in the yellow square are magnified and shown in B to E. B: Detection of *Sost* mRNA with an antisense probe by ISH (dark purple). C: Negative control for ISH with *Sost* sense probe. D: Detection of sclerostin with anti-sclerostin antibody by IHC (green color). E: Negative control for IHC with normal rabbit IgG. Nuclei were stained with methyl green in B (light green) and C (light green) and with 4′ , 6-diamidino-2-phenylindole in D (blue) and E (blue). The images were taken from the epithelial side (osseous layer) of scale.

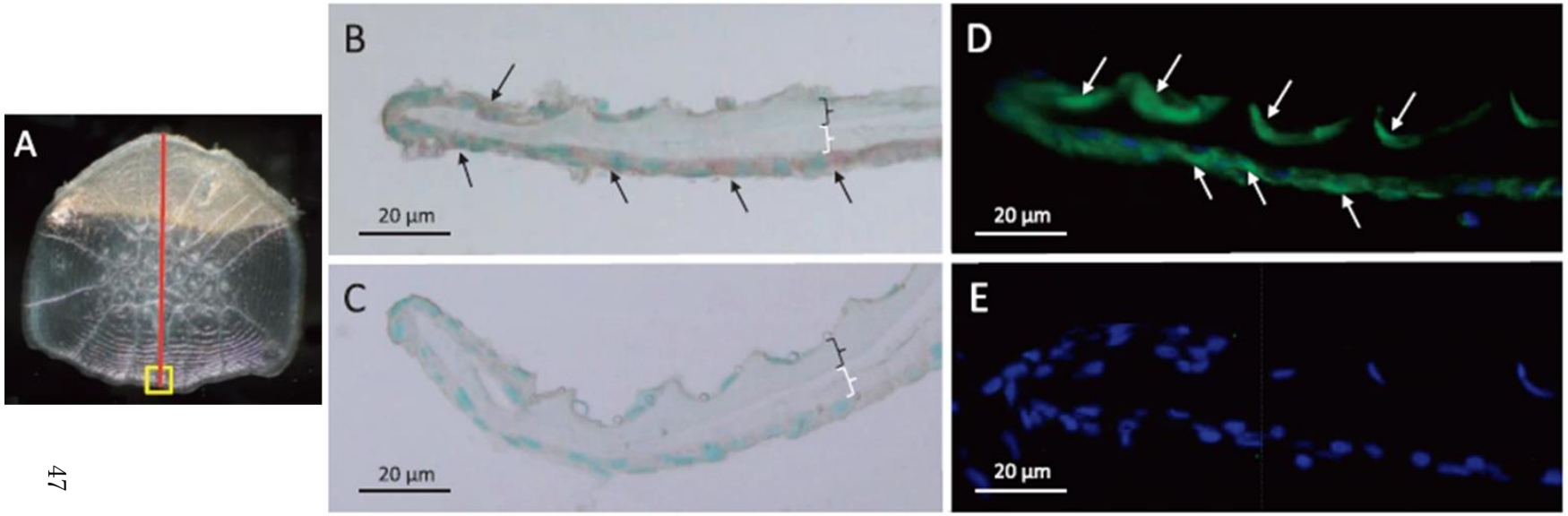

Fig. 8. Detection of *Sost*/sclerostin in the peripheral area of the regenerating scales with cryosections by *in situ* hybridization (ISH) and immunohistochemistry (IHC). A: Binocular view of a regenerating scale on day 15. The parts corresponding to the area in the yellow square in cryosections are magnified and shown in B to E, in which the epidermis and dermis sides are shown on the upper and lower sides, respectively. The cryosections were cut along the red line. B: Detection of *Sost* mRNA with an antisense probe by ISH (brownish-purple). Osseous and fibrous layers are indicated by black and white curly braces respectively. C: Negative control for ISH with a *Sost* sense probe. Osseous and fibrous layers are indicated by black and white curly braces respectively. D: Detection of sclerostin with anti-sclerostin antibodies by IHC. Positive staining is indicated by a green color (arrows). E: Negative control for IHC with normal rabbit IgG. Nuclei were stained with methyl green in B (light green) and C (light green) and with 4′, 6-diamidino-2-phenylindole in D (blue) and E (blue).

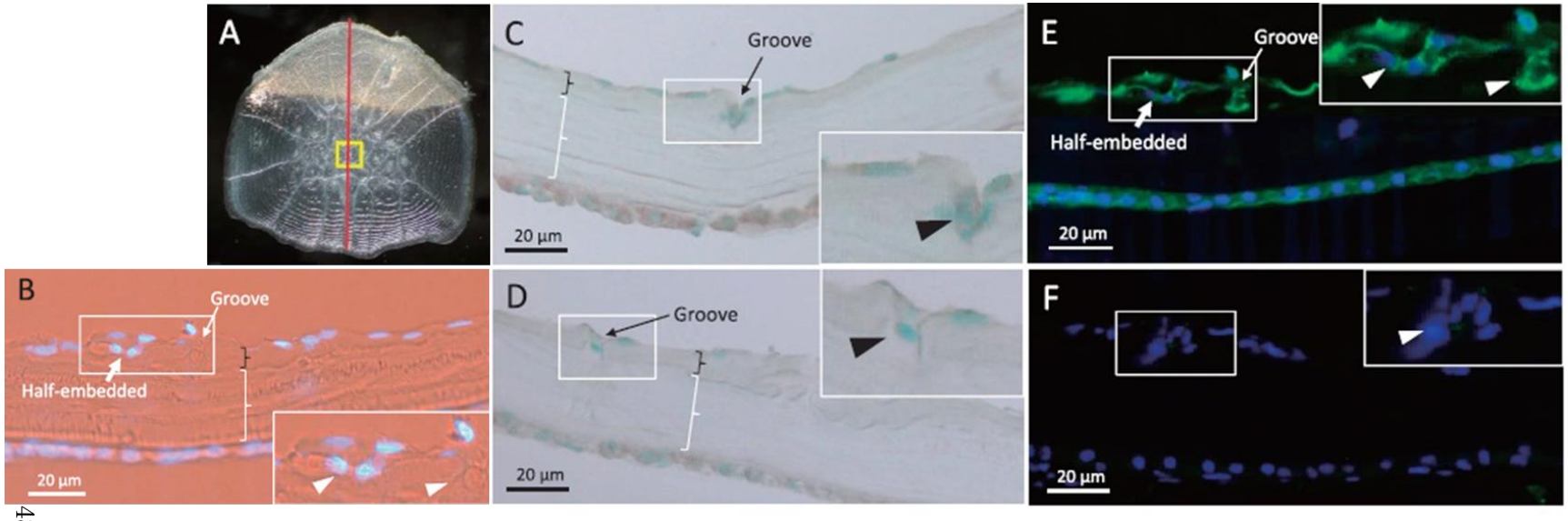

Fig. 9. Detection of *Sost*/sclerostin in the central area of regenerating scales with cryosections by *in situ* hybridization (ISH) and immunohistochemistry (IHC). A: Binocular view of a regenerating scale on day 15. The parts corresponding to the area in the yellow square in cryosections are magnified and shown in B to F. The cryosections were cut along the red line. The inset is a magnified view of the area in the square (B to F). B: Bright-field observation of the cryosection. C: Detection of *Sost* mRNA with an antisense probe by ISH (brownish-purple). D: Negative control for ISH with a *Sost* sense probe. E: Same field of view as B, observed with fluorescent microscopy. Sclerostin was detected with anti-sclerostin antibodies by IHC (green). F: Negative control for IHC with normal rabbit IgG. Nuclei were stained with methyl green in C (light green) and D (light green) and with 4′, 6-diamidino-2-phenylindole (DAPI) in B (pale blue), E (blue), and F (blue). The nuclei appear pale blue in B due to the fact that the blue fluorescent color of DAPI and the visible light image are superimposed.

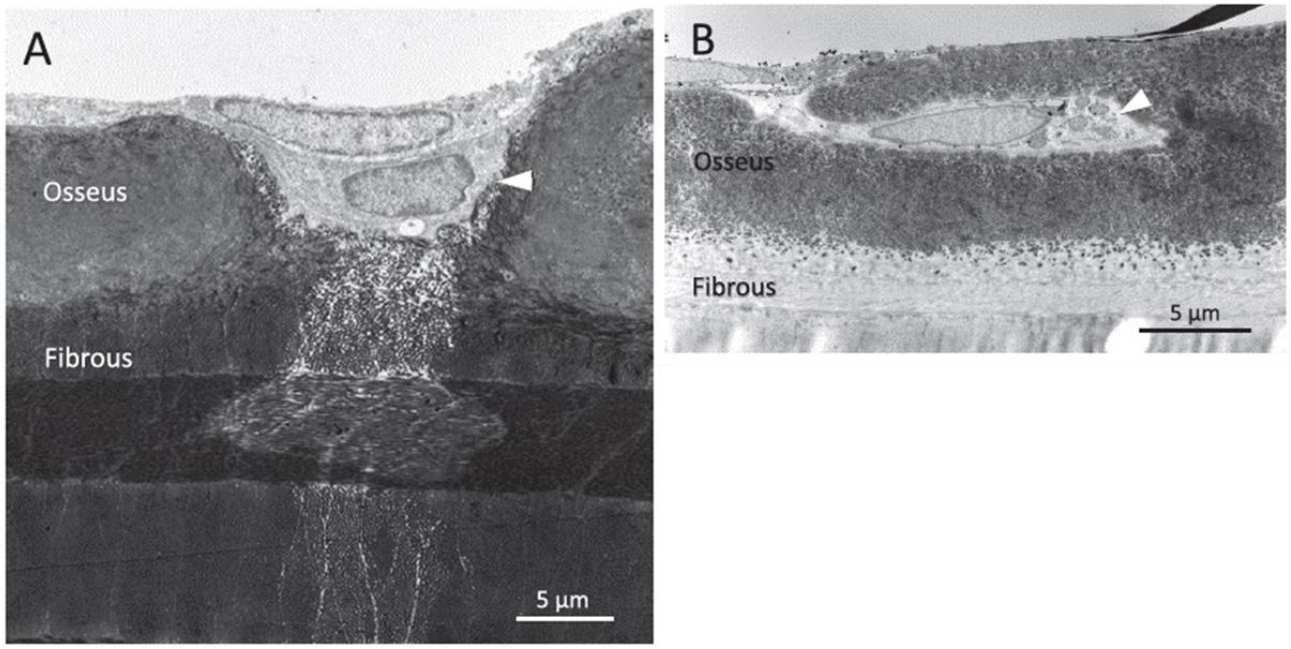

Fig. 10. Electron microscopic observation of the half-embedded cells in osseous layer of regenerating scale. A: A decalcified scale. A half-embedded cell (arrow head) in a groove observed between the mineralized matrices. A part of fibrous layer is shown in the bottom half of the panel; plywood-like collagen fibers are stained by tannic acid. B: An un-decalcified scale. A half-embedded cell (arrow head) observed in the mineralized matrix.

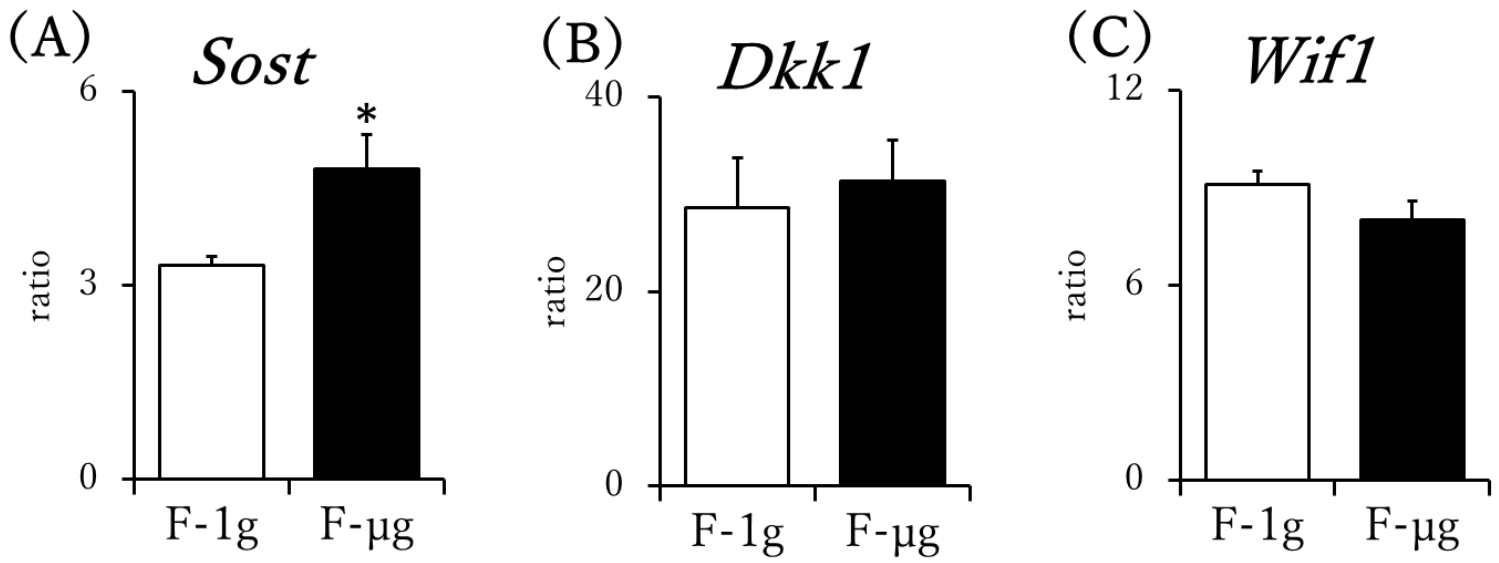

Fig. 11. Expression analyses of Wnt inhibitors *Sost*, *Dkk1*, and *Wif1* in the regenerating scales of goldfish under microgravity by quantitative RT-PCR. *Ef1 α* gene was used for normalization of respective gene expression. Data represent the mean ± S.E.M. ($n = 4$). * $p < 0.05$ versus control.

Table 2. Primer sequences used for quantitative real-time PCR

Target gene	Forward sequence (5’ → 3’)	Reverse sequence (5’ → 3’)
Sost	CCGATTACCGCTGCATTCCT	CGTCCGATTGGTTGTGATGG
Dkk1	AAGCACAAGAGGAAAGGCACCCAT	TTAGTGTCTCTGGCAAGTGTGCAG
Wif1	TGCCGAAGAGCAAGGAAGC	TCCTGAAGTCGTGTGTGAATGGGG
Ef1 α	ATTGTTGCTGGTGGTGTTGG	GGCACTGACTTCCTTGGTGA

IV. Osteoblastic and osteoclastic response to hypergravity and microgravity in goldfish scales as a bone model

Introduction

Bone is a dynamic hard tissue that consists of three types of cells: osteoblasts, osteoclasts, and osteocytes (Civitelli, 2008; Schaffler and Kennedy, 2012; Chen *et al.*, 2018). Osteoblasts are bone-forming cells that secrete bone matrix to form hard bone, while osteoclasts are bone-resorbing cells that elute bone matrix by several enzymes. Physical stimulation functions directly or indirectly in these bone cells and plays an important role in the regulation of bone remodeling (Carmeliet *et al.*, 2001; Civitelli, 2008). However, the process of translating the physical stimuli into biological responses, called *mechanotransduction*, is currently poorly understood due to the lack of a highly sensitive *in vitro* model system. Also, bone matrix plays an important role in the response to physical stimuli (Harter *et al.*, 1995; Owan *et al.*, 1997; Hoffler *et al.*, 2006). It is known that $\alpha 5 \beta 1$ integrin, which is involved in the adhesion of cells to the bone matrix, plays an important role in mechanotransduction (Watabe *et al.*, 2011). Therefore, in order to accurately analyze the bone metabolic response to physical stimuli such as hypergravity and microgravity, an *in vitro* bioassay system coexisting with

osteoclasts, osteoblasts, and bone matrix has been desired.

On the other hand, the teleost scale is a unique calcified bone that has osteoblasts, osteoclasts, and two layers of calcified matrix, i.e., a fibrillary layer that possesses both a thick partially calcified layer and a bony layer, which is a thin calcified external layer (Bereiter-Hahn and Zylberberg, 1993; Suzuki *et al.*, 2007; Ohira *et al.*, 2007; Ikegame *et al.*, 2019). Calcified bone matrix containing type I collagen (Zylberberg *et al.*, 1992), osteocalcin (Nishimoto *et al.*, 1992), and hydroxyapatite (Onozato and Watabe, 1979) exists in teleost scales, which is quite similar to mammalian bone. Furthermore, our group recently found that osteocyte-like cells are present in goldfish scales (Yamamoto *et al.*, 2020b). Osteocytes are known to be major sensors for the mechanical loading of mammalian bone (Tatsumi *et al.*, 2007; Lin *et al.*, 2009; Schaffler and Kennedy, 2012; Alford *et al.*, 2015; Smith, 2020); therefore, fish scales can be used to analyze physical stimuli.

In this study, a previously developed scale organ culture system (Suzuki *et al.*, 2000; Suzuki and Hattori, 2002; Omori *et al.*, 2012) was used to investigate the effects of hypergravity with a centrifuge and simulated ground microgravity (g-μG) with a three-dimensional (3D) clinostat on osteoblasts and osteoclasts. To

confirm the results obtained by simulated microgravity, biological space experiments were conducted to investigate the effect of flight microgravity (f-μG) on bone cells. The present study is the first to morphologically demonstrate the effects of hypergravity and microgravity on osteoclasts, indicating that the Wnt signaling pathway has an essential function in the response of both osteoblasts and osteoclasts to both hypergravity and microgravity.

Materials and Methods

Animals

Goldfish (*Carassius auratus*) were commercially obtained from Higashikawa Fish Farm (Yamatokoriyama, Nara, Japan) and artificially fertilized from a pair of male and female goldfish (20–30 g) at the Laboratory of Fish Culture, Tokyo University of Marine Science and Technology. Hatched fish were fed brine shrimp feed as bait, and then a commercially available compound feed to grow up. After that, fish were fed a commercial pellet feed for sea bream every morning and maintained in fresh water at a temperature of 26°C. Growing fish (length: 12–15 cm) were transferred to Tokyo Medical and Dental University and Noto Marine Laboratory of Kanazawa University to use for *in vitro* mRNA expression analysis and morphological studies.

All experimental procedures were carried out according to the Guide for the Care and Use of Laboratory Animals prepared by Tokyo Medical and Dental University and Kanazawa University.

Preparation of regenerating goldfish scales

Teleost fish scales regenerate after being removed. It was previously reported that bone formation in regenerating scales is very similar to osteogenesis in the calvaria (mammalian head bone) (Yoshikubo *et al.*, 2005). Osteoblast activity in regenerating scales was also significantly higher than in normal scales (Yoshikubo *et al.*, 2005; Suzuki *et al.*, 2009; Thamamongood *et al.*, 2012). Therefore, I used regenerating scales to investigate the effects of hypergravity by centrifugation and simulated ground microgravity (g-μG) on osteoclasts and osteoblasts.

The grown scales were removed from goldfish anesthetized with 0.03% Ms-222 (Sigma-Aldrich) to allow scale regeneration. The scales were removed, one on each of the two horizontal lines, using sharp forceps. The goldfish were then bred at 26℃ for a 12-hour light/12-hour dark cycle (lit at 8 a.m.). On the 12th day after scale removal, goldfish were bred in water using an anti-infection control reagent, Green F Gold (Japan Pet Design, Tokyo Japan). Subsequently, on day 14, regenerating scales from goldfish on ice were sterilized with low-concentration hypochlorous acid and fungizone solutions and then immersed in Leibovitz's L-15 medium (Invitrogen) containing 10% FCS (Nichirei Biosciences), 200 μg/mL

kanamycin, 100 μg/mL streptomycin, and 100 U/mL penicillin.

Hypergravity and simulated g-μG treatments of regenerating goldfish scales

Sterilized scales were placed in 96-well plates (one scale per well). The lines on the left were used as the experimental group, and the lines on the right were used as the control group. During loading, various parallel experiments were conducted using 10 goldfish. A 96-well plate containing the scale was loaded into 3-gravity (3G) for one day using a centrifuge machine (LIX-130, Tomy Digital Biology) (Suzuki *et al.*, 2008b). After finishing centrifugation, the incubated scales were placed in RNAlater (Sigma-Aldrich) and frozen at -80℃ for mRNA analysis.

For g-μG simulated with 3D clinostat processing, the regenerating scales were prepared as above and placed in a 96-well plate (one scale per well). In this study, I performed different parallel experiments with 10 goldfish. Plates containing scales were processed to simulate g-μG using a 3D clinostat (Toray Engineering) for one day (Fig. 12). After using a 3D clinostat, the scales were stocked in RNAlater (Sigma-Aldrich) at -80℃ until the mRNA expression was analyzed.

Changes in osteoblastic and osteoclastic marker mRNA expression in

hypergravity- and simulated g-μG-treated scales

Osteoblastic (*collagen type I alpha 1: Col1a1; Dickkopf-related protein 1: Dkk1; osteocalcin: Ocn; osteoprotegerin: Opg; receptor activator of NFκB ligand: Rankl; Wnt inhibitory factor 1: Wif1*) and osteoclastic (*cathepsin K: Ctsk; cellular-Src: c-Src; integrin beta-3: Itgb3; osteoclast stimulatory transmembrane protein: Oc-stamp; tartrate-resistant acid phosphatase: Trap*) marker mRNAs that responded to hypergravity and simulated g-μG were examined.

Total RNA isolation and cDNA synthesis were performed using a kit (Qiagen GmbH) in accordance with the manufacturer's instructions (Suzuki *et al.*, 2011; Ishizu *et al.*, 2018). Each quantitative real-time PCR reaction was performed using a real-time PCR device (Mx3000p, Stratagene). In the PCR reaction, a cDNA template was combined with appropriate primers and SYBR Premix Ex Taq (Takara Bio) (Ikegame *et al.*, 2019). The conditions for PCR amplification were as follows: 40 cycles of denaturation for 10 seconds at 95°C and annealing for 40 seconds at 60°C.

Elongation-factor 1α (*Ef-1α*) was used for normalization in qPCR experiments. The PCR primer sequences used in the current study are shown in Table 3.

Morphological analysis of osteoclasts in hypergravity- and simulated g-μG-treated scales

Treatment of hypergravity and simulated g-μG on the regenerating scales: After sterilizing the regenerating scales by the method described above, they were put into 96-well plates (one scale per well) with Leibovitz's L-15 medium (Invitrogen) containing 10% FCS (Nichirei), 200 μg/mL kanamycin, 100 μg/mL streptomycin, and 100 U/mL penicillin. In 3G loading, various parallel experiments were conducted using 10 goldfish. The 96-well plates containing the scales were loaded into 3G for 86 hours (Suzuki *et al.*, 2008b) using a centrifuge machine (LIX-130, Tomy Digital Biology). This loading time was set to be the same as that of a previous biological space experiment (Ikegame *et al.*, 2019). After centrifugation, the scales were fixed overnight at 4℃ with 4% PFA in 0.1 M phosphate buffer (pH 7.4). Next, the fixed samples were transferred to PBS. Unloading was done by 3D clinostat machine (Toray Engineering). For the simulated g-μG process, the regenerating scales were also prepared as described above, placed in a 96-well plate (one scale per well), and processed in a 3D clinostat for 86 hours. The various parallel experiments were performed with 10

goldfish, as had been done with hypergravity loading by centrifuge. After unloading with a 3D clinostat, the scales were fixed overnight at 4°C with 4% PFA in 0.1 M phosphate buffer (pH 7.4). Next, the fixed samples were placed in PBS.

Actin staining: The fixed specimens were incubated with 0.1% Triton X-100 for 10 minutes. F-actin was stained with 1% Alexa Fluor® 488 phalloidin (Molecular Probes) in PBS in the dark at 4°C for 4 days. After washing with PBS, nuclear staining was performed using DAPI (Dojindo) and observed with a fluorescence microscope (BX51, Olympus).

TRAP staining: The fixed specimens were stained for TRAP enzyme activity in accordance with the modified method of Cole and Walters (1987). Briefly, the scales were incubated in a solution containing 50 mM tartrate, fast red violet (0.7 mg/ml; Sigma-Aldrich) as a diazonium-coupling salt, and naphthol AS-BI (0.1 mg ml; Sigma-Aldrich). The specimens were observed under a microscope (SZX10, Olympus).

Histomorphometry: Using randomly selected scales, histomorphometric analysis was performed in six 0.31 mm^2 observation areas. Average measurements from the six areas were considered as representative of each scale. The number of osteoclasts per mm^2 was recorded, and the average number of osteoclasts per

multinucleated osteoclast and the proportion of osteoclasts with actin rings were calculated. The ratio of the width of the grooves in the center of each groove, the size of the actin ring, and the percentage of groove lengths covered with actin rings were measured by NIH Image J (https://imagej.nih.gov/ij/) software.

Biological space experiment at the International Space Station

The goldfish were anesthetized, and sharpened forceps were used to extract the scales, one on each of the two horizontal lines. The goldfish were then bred at 26°C for a 12-hour light/12-hour dark cycle (lit at 8 am every day). On the 12th day after the scales were removed, goldfish were bred in water using an anti-infection reagent, Green F Gold (Nippon Pet Design). The next day, 8 regenerating scales were collected from each goldfish ($n = 40$) to measure alkaline phosphatase (ALP) for osteoblast activity ($n = 4$) and TRAP for osteoclast activity ($n = 4$). As mentioned above, individual goldfish with similar ALP and TRAP activity were selected from the 40 prepared goldfish. Subsequently, on day 14, regenerating scales were sterilized with hypochlorous acid and fungizone solutions and transferred to Leibovitz's L-15 medium (Invitrogen) containing 10% FCS (Nichirei Biosciences), 200 μg/mL of kanamycin, 100 μg/mL of

streptomycin, and 100 U/mL of penicillin. Sterilized goldfish scales were packed in a Cell Experiment Small Chamber culture chamber (Chiyoda Corporation) (60 scales/chamber) and stored at 4℃ for 86 hours before space shuttle STS-132 (ULF4) was launched to the ISS. The culture chambers were kept at between 2.5 and 4.0℃ and sent to the ISS *via* the Space Shuttle Atlantis (STS-132) (Yano, 2011) (Fig. 13). After arriving at the ISS, they were cultured for 86 hours under microgravity at the CBEF (Yano, 2011). The CBEF is equipped with a centrifuge for processing samples with a single gravity [artificial microgravity in flight (f-1G)] (Yano *et al.*, 2012). The facility is capable of culturing biological samples in a temperature range of 15 to 40℃ (Yano *et al.*, 2012). During culture in the CBEF, the incubation chamber placed under microgravity (f-μG) and the 1G section (f-1G) of the CBEF were incubated in the Measurement Experiment Unit (MEU) at between 21.9 and 22.0℃ (Yano, 2011; Yano *et al.*, 2012). The culture chambers were treated with 1G gravity in the 1G section but were maintained without gravity treatment in the microgravity section. After the process of incubation, the culture chambers were removed from the MEU. The medium in the culture chambers was then replaced with RNAlater (Sigma-Aldrich) for gene expression analysis. The above procedure was performed precisely by astronaut Soichi

Noguchi of the Japan Aerospace Exploration Agency. The RNAlater-treated scales were stored at -96℃ until STS-132 returned to the Kennedy Space Center in Florida, and then its biological properties as determined by space experiments were analyzed.

Global gene expression and pathway analysis

In order to extract genes that respond to microgravity, the deposited RNA-sequencing (RNA-seq) read DRA008502 was reanalyzed. The RNA-seq raw reads were deposited at the DNA Data Bank of Japan (DDBJ) under accession number DRA009118. Details of such methods for building libraries, sequencing, *de novo* transcriptome assembly, mapping, and quantification followed those of previous reports (Ikegame *et al.*, 2019). Differentially expressed genes (DEGs) with a logarithm of twofold change > |0.58| from the comparison of f-1G and f-μG were selected. Using Ingenuity® Pathway Analysis tools (Qiagen), the DEGs were further analyzed (Tabuchi *et al.*, 2006).

Statistical analysis

All results are presented as the means ± SE. The statistical significance of

differences between the control and experimental groups was assessed using the paired Student's *t*-test. In all cases of the present experiments, the significance level selected was $p < 0.05$.

Results

Effect of centrifuge hypergravity (3G) on the mRNA expression of osteoclast and osteoblast markers

In Figures 14 and 15, the results of osteoclasts and osteoblasts by 3G loading are shown. The expression of osteoclastic markers *Ctsk* and *Trap* were reduced significantly by 3G loading. By 3G loading, the mRNA expressions of *Oc-stamp*, *Itgb3*, and *c-Src* were not changed significantly. On the other hand, the mRNA expressions of osteoblastic markers *Ocn*, *Rankl*, and *Opg* were significantly upregulated by 3G loading on scale. *Dkk1* mRNA expression was significantly downregulated by 3G loading. However, with 3G treatment, the values of *Col1a1* and *Wif1* mRNA expression were not changed as compared with the control values in the regenerating scales.

Effect of simulated g-μG on mRNA expression of osteoclastic and osteoblastic markers using a 3D clinostat

In Figures 16 and 17, the effects of simulated g-μG on osteoclasts and osteoblasts are shown. All osteoclastic markers (*Ctsk*, *Trap*, *Oc-stamp*, *Itgb3*, and *c-Src*) investigated in this study were significantly upregulated. On the other hand, in osteoblasts, the expression of *Col1a1* mRNA was significantly suppressed under simulated g-μG, but the expression of *Ocn* mRNA was not altered by simulated g-μG loading. The expression of *Rankl* mRNA was upregulated remarkably, although the expression of *Opg* mRNA was not changed by simulated g-μG treatments. The mRNA expression of *Wif1* and *Dkk1* was increased significantly.

Changes in the ratio of Rankl/Opg under hypergravity and simulated g-μG

The *Rankl/Opg* ratios were analyzed to examine the regulation of osteoclastic function (Fig. 18). The ratio of *Rankl/Opg* was significantly reduced by 3G hypergravity. However, under simulated g-μG, the *Rankl/Opg* ratio was significantly upregulated.

Morphological changes in osteoclasts by hypergravity and simulated g-μG loading

Osteoblasts were not significantly changed by either hypergravity (3G) or simulated g-μG treatment, at least under current conditions. In this study, I

focused on osteoclasts, investigating the morphological changes of osteoclasts in detail.

Osteoclasts with actin rings were observed primarily along the scale grooves (Fig. 19A–19D). In these osteoclasts, both the number of actin rings and the percentage of lengths of grooves associated with the actin rings were remarkably lower in the 3G-loaded scales than in the control scales (Fig. 19E and 19F). However, the actin ring size, the number of nuclei in multinucleated osteoclasts, and number of osteoclasts were not changed significantly (Fig. 19G–19I).

Under simulated g-μG loading, the groove widths of scales were enlarged significantly more than in the control scales (Fig. 20A–20C).

The osteoclasts appeared larger, and the number of nuclei of multinucleated osteoclasts was upregulated remarkably by simulated g-μG treatment (Fig. 20F). The number of mononuclear osteoclasts was downregulated (Fig. 20D) in correlation with this increase in the number of nuclei in multinucleated osteoclasts (Fig. 20F). In addition, there was no significant difference in the number of multinucleated osteoclasts between the simulated g-μG group and the control group (Fig. 20E). The percentage of actin ring-positive multinucleated osteoclasts and the actin ring size in simulated g-μG loading scales were upregulated

significantly (Fig. 20G and 20H) more than in the control scale. In addition, the lengths of grooves associated with the actin rings were upregulated because actin rings were mostly observed along scale grooves under simulated g-μG loading (Fig. 20I).

Changes in osteoclastic markers during space flight

During the space flight experiment, mRNA expressions of the osteoclastic markers *Oc-stamp*, *Itgb3*, and *c-Src* were elevated (Fig. 21). There was a significant difference in the expression of *Itgb3* mRNA between f-μG and f-1G.

Global gene expression and pathway analysis during space flight

The obtained data were enriched with Ingenuity® Pathway Analysis tools to identify standard routes associated with space flight. As a result, it was predicted that the Wnt/β-catenin pathway is involved in the f-μG response.

Figure 22 shows the canonical Wnt/β-catenin pathway, in which green-shaded shapes indicate downregulated genes by f-μG. During space flight, the canonical Wnt/β-catenin pathway–related genes were downregulated. In particular, the expression of β-catenin-related genes was suppressed under f-μG.

Discussion

In this study, it was found that osteoclasts and osteoblasts in goldfish scales quite sensitively respond to hypergravity and simulated g-μG because the *in vitro* scale organ culture systems—which consist of osteoclasts, osteoblasts, and an intact bone matrix—were used for analyzing gravities. This is the first study to simultaneously examine the functions of both osteoclasts and osteoblasts in response to hypergravity by centrifugation and simulated g-μG by 3D clinostat, respectively. In other words, it was found that 3G loading changes the mRNA expression of osteoclast and osteoblast markers and functions to induce bone formation (Figs. 14 and 15). On the other hand, in simulated g-μG by 3D clinostat, the expression of osteoclastic marker mRNA was significantly upregulated (Fig. 16), but the expression of osteoblastic marker mRNA was downregulated (Fig. 17). Under simulated g-μG, the markers indicated above functioned to induce bone resorption in goldfish scales. Moreover, morphological observations indicated that osteoclastic inactivation was induced by 3G loading (Fig. 19), and osteoclastic

activation was enhanced under simulated g-μG by 3D clinostat (Fig. 20). These changes in goldfish scale osteoclasts and osteoblasts due to hypergravity and simulated g-μG by 3D clinostat were consistent with those observed in mammalian *in vivo* investigations (Kawao *et al.*, 2016; Chatziravdeli *et al.*, 2019; Smith, 2020). I concluded that the *in vitro* organ culture system of the goldfish scale is an excellent model for analyzing bone metabolism under gravity.

Several investigations of hypergravity using mammalian osteoblasts have been reported. Osteoblastic responses for high-G loading of 5 to 50 G have been studied, and the activation of osteoblasts by high-G loading has also been reported (Gebken *et al.*, 1999; Saito *et al.*, 2003; Searby *et al.*, 2005; Zhou *et al.*, 2015). Similarly to mammalian osteoblasts, scale osteoblasts (Gebken *et al.*, 1999; Saito *et al.*, 2003; Searby *et al.*, 2005; Zhou *et al.*, 2015) responded sensitively and were activated by relatively low-G (3G) loading in my study (Fig. 15). Mammalian osteoclasts did not show a clear response to hypergravity (Nemoto and Uemura, 2000). Specifically, osteoclasts isolated from rabbits were cultured on ivory and then exposed to 30 G for 2 or 18 hours by placing the culture tubes in a swinging bucket rotor. As a result, no effect of hypergravity was observed on the number of activated osteoclasts with actin ring formation (Nemoto and Uemura, 2000). The

effects of various gravity loading conditions on mammalian osteoclasts need to be considered. Interestingly, in an *in vivo* investigation of mice, the mineral content of the trabecular bone was increased significantly by 3G loading centrifugation, and bone formation was induced (Kawao *et al.*, 2016). Therefore, it was indicated that osteoclasts and osteoblasts respond to hypergravity without the application of high gravity. For this reason, an organ culture system using fish scales can analyze bone metabolism in a state close to that *in vivo* because the scale osteoclasts and osteoblasts responded to 3G hypergravity loading in a manner similar to that of mammals in *in vivo* studies. In addition, under simulated g-μG by 3D clinostat, osteoclastic and osteoblastic responses of mammalian cell cultures did not agree with those of the *in vivo* investigation during space flight (Makihara *et al.*, 2008; Chatziravdeli *et al.*, 2019; Smith, 2020). It has been reported that the activation of osteoclasts did not occur due to the suppression of *Rankl* mRNA expression under simulated g-μG by 3D clinostat (Makihira *et al.*, 2008). Interestingly, my ground-based results of the simulated g-μG by 3D clinostat were in good agreement with the results of space experiments (Ikegame *et al.*, 2019; Smith, 2020). Considering these results and those obtained in the present study, the organ culture of fish scales is very similar to that of *in vivo* studies of mammals

and shows an excellent response to both hypergravity and microgravity.

Osteoclasts are known to be regulated by interaction with osteoblasts (Kondo *et al.*, 2001; Kearns *et al.*, 2008; Lacey *et al.*, 2012). In other words, osteoclasts (active type) multinucleated by the fusion of pre-osteoclasts are produced by binding RANKL expressed in osteoblasts to RANK existing in osteoclasts. Additionally, OPG produced by osteoblasts is a decoy receptor for RANKL and, thereby, suppresses osteoclastogenesis (Kubota *et al.*, 2009; Silva and Branco, 2011; Lacey *et al.*, 2012). As described above, osteoclastic activation is regulated by RANK, RANKL, and OPG systems. Therefore, in this study, we analyzed the expression of genes encoding these molecules. The *Rankl/Opg* ratio was reduced significantly by 3G hypergravity, while the ratio was increased by simulated g-μG by 3D clinostat (Fig. 18). Therefore, this difference depends on the fact that *Opg* expression was increased by hypergravity (Fig. 15), but simulated g-μG was not (Fig. 17). Therefore, the Wnt/β-catenin signaling pathway inhibitors (*Wif1* and *Dkk1*), which are important signaling pathways that regulate OPG expression (Kubota *et al.*, 2009; Silva and Branco, 2011), were analyzed in this study. The expression of *Dkk1* mRNA was reduced by 3G loading with a centrifuge machine (Fig. 15), while the expression was significantly increased under simulated g-μG

by 3D clinostat (Fig. 17). The expression of *Wif1* mRNA was significantly increased in simulated g-μG by 3D clinostat (Fig. 17), but it did not change under 3G hypergravity conditions (Fig. 15).

It was found that the expression of *Rankl* mRNA is enhanced by both hypergravity and simulated g-μG by 3D clinostat. This result indicates that the *Rank1* gene may be generally sensitive to changes in gravity. Following this idea, the differentially expressed genes were investigated in both microgravity by 3D clinostat and hypergravity by centrifugation, and it was shown that the expression of the G protein–coupled receptor OR12D3 is suppressed by both microgravity and hypergravity as well as levels of three non-coding RNAs (RNUD-1, SNORD63, and AC083843.1) (Thiel *et al.*, 2017).

In order to confirm the results obtained by simulated g-μG treatments by 3D clinostat, biological space experiments were performed, and the influence of f-μG on bone metabolism was investigated. During space flight, the mRNA expressions of osteoclastic markers *Oc-stamp*, *Itgb3*, and *c-Src* were increased. Changes in gravity alter the expression levels of various genes, and interactions among bone marker genes have been reported to play an important role in the cellular response to gravity loading or unloading (Cavanagh *et al.*, 2005; Smith,

2020). Therefore, the effect of cosmic microgravity on gene expression in fish scales (bone model) was investigated comprehensively. The results showed that the Wnt/β-catenin pathway was involved in the response of bone cells in the bone model fish scale to f-μG. In particular, the Wnt/β-catenin pathway has been shown to play an important role in the response of bone cells to gravity (Lin *et al.*, 2009). Several genes involved in the Wnt/β-catenin pathway were downregulated during space flight. These results were in agreement with the simulated g-μG results (Figs. 16–18).

Due to the distribution of osteoblasts and osteoclasts on the surface, fish scales have the helpful feature of facilitating a full morphological analysis (Kobayashi *et al.*, 2016; Suzuki *et al.*, 2016; Ikegame *et al.*, 2019). The size of osteoclasts and the number of nuclei in multinucleated osteoclasts were significantly upregulated more than those of 1G control scales (Fig. 20). Most osteoclasts of the active form were distributed along the edges of the scale grooves (Fig. 20). Interestingly, it was reported that RANKL-producing cells were distributed in contact with multinucleated osteoclasts in the grooves of the regenerating scales (Yamamoto *et al.*, 2020a). This strongly implied that osteoclasts were activated by RANKL that was secreted from RANKL-producing cells. Increased *Oc-stamp* mRNA

expression associated with osteoclast multinucleation (Yamamoto *et al.*, 2020b) (Fig. 16) under simulated g-μG treatment by 3D clinostat was supported by the above results. So far, there have been several reports on the activation of osteoclasts under microgravity, including simulated g-μG (Rucci *et al.*, 2007; Tamma *et al.*, 2008; Smith, 2020). However, no studies have investigated in detail the morphological changes of osteoclasts under hypergravity. This is the first study to morphologically show hypergravity and g-μG responses to osteoclasts using the same method.

In addition to the response to gravity changes, it was previously shown that low-intensity pulsed ultrasound (LIPUS) stimulation promoted scale regeneration in goldfish (Hanmoto *et al.*, 2017). Using LIPUS, the expression of osteoblastic genes in the scales of zebrafish was upregulated, and the apoptosis of osteoclasts was induced at the same time (Suzuki *et al.*, 2016). In addition, previous studies have shown that the activities of both osteoclasts and osteoblasts change in response to hypergravity on the scales of medaka (Yano *et al.*, 2013). Current research results, along with the above findings using fish scales, provide evidence that the organ culture system of teleost fish scales, in which osteoclasts and osteoblasts coexist on the intact bone matrix and are sensitive to gravitational

changes, is a suitable experimental system for investigating the responses of bone cells to changes in gravity during space flight.

Fig. 12. Photograph of three-dimensional clinostat. Three-dimensional (3D) clinostats are valuable devices for simulating micro-gravity environments. By rotating the sample three-dimensionally, the sample can eliminate the dynamic stimulus of gravity in all directions.

Fig. 13. Space shuttle STS-132 launched to the International Space Station. On May 14, 2010, the Space Shuttle STS-132 (ULF4) carrying our specimens (goldfish scales) was launched on the ISS. JAXA astronaut Soichi Noguchi works at the International Space Station.

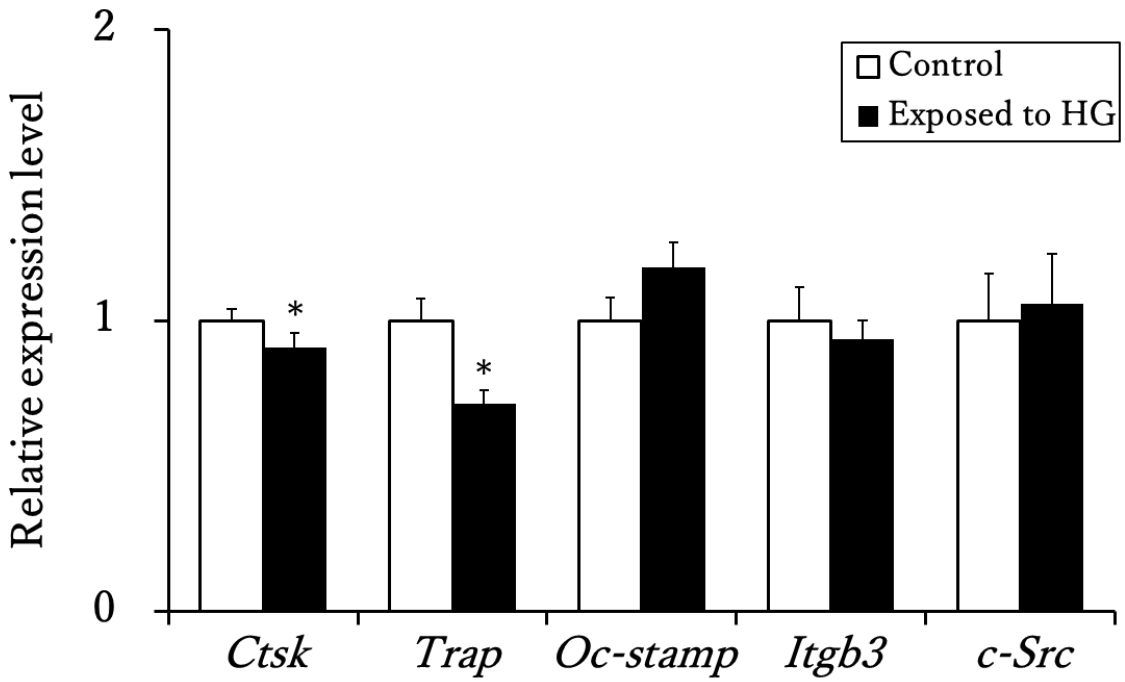

Fig. 14. Effects of hypergravity (HG) on expression of osteoclastic marker genes. The value for the control sample was set as 1 for each gene. Data represent the mean ± S.E.M. ($n = 10$). * $p < 0.05$ (Paired t-test).

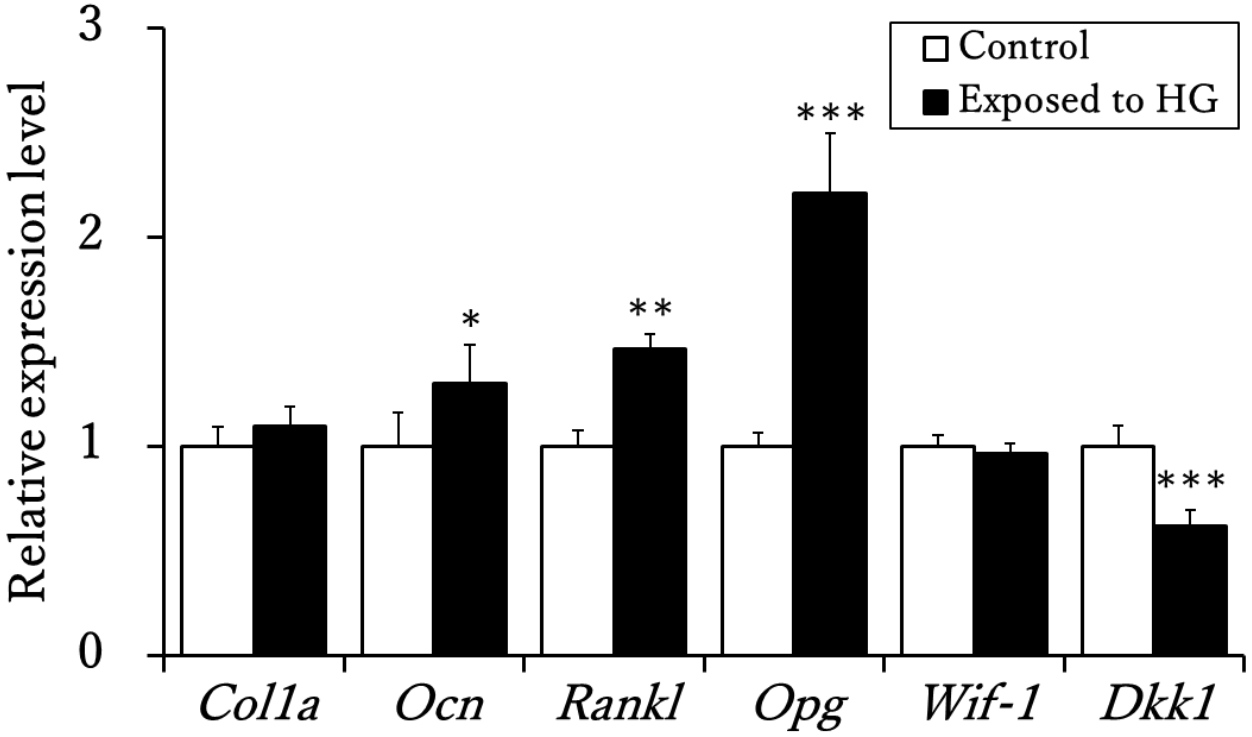

Fig. 15. Effects of hypergravity (HG) on expression of osteoblastic marker genes. The value for the control sample was set as 1 for each gene. Data represent the mean ± S.E.M. ($n = 10$). * $p < 0.05$ (Paired t-test), ** $p < 0.01$ (Paired t-test), and *** $p < 0.001$ (Paired t-test).

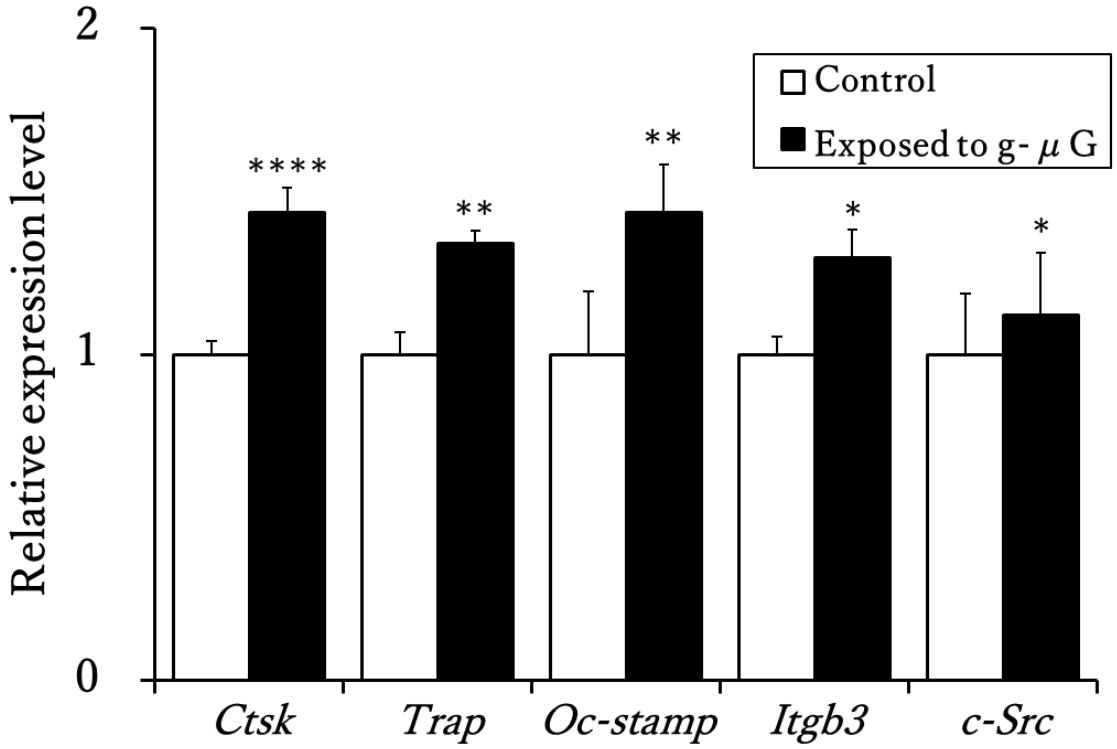

Fig. 16. Effects of simulated ground microgravity (g-μG) on expression of osteoclastic marker genes. The value for the control sample was set as 1 for each gene. Data represent the mean ± S.E.M. ($n = 10$). * $p < 0.05$ (Paired t-test), ** $p < 0.01$ (Paired t-test), and **** $p < 0.0001$ (Paired t-test).

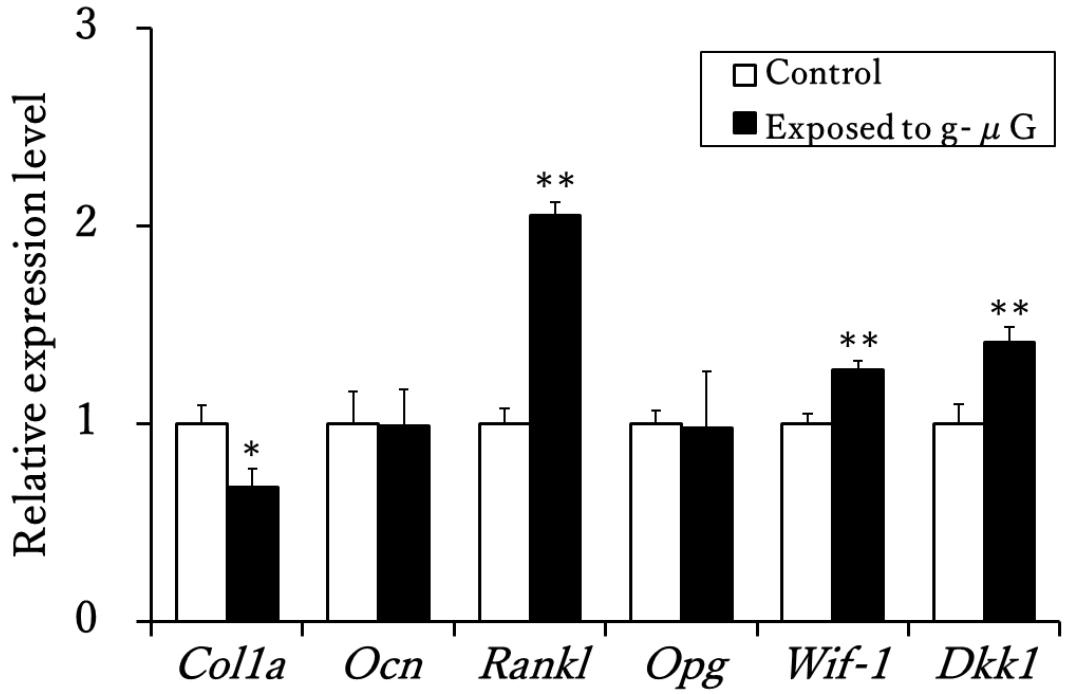

Fig. 17. Effects of simulated ground microgravity (g-μG) on expression of osteoblastic marker genes. The value for the control sample was set as 1 for each gene. Data represent the mean ± S.E.M. ($n = 10$). * $p < 0.05$ (Paired t-test) and ** $p < 0.01$ (Paired t-test).

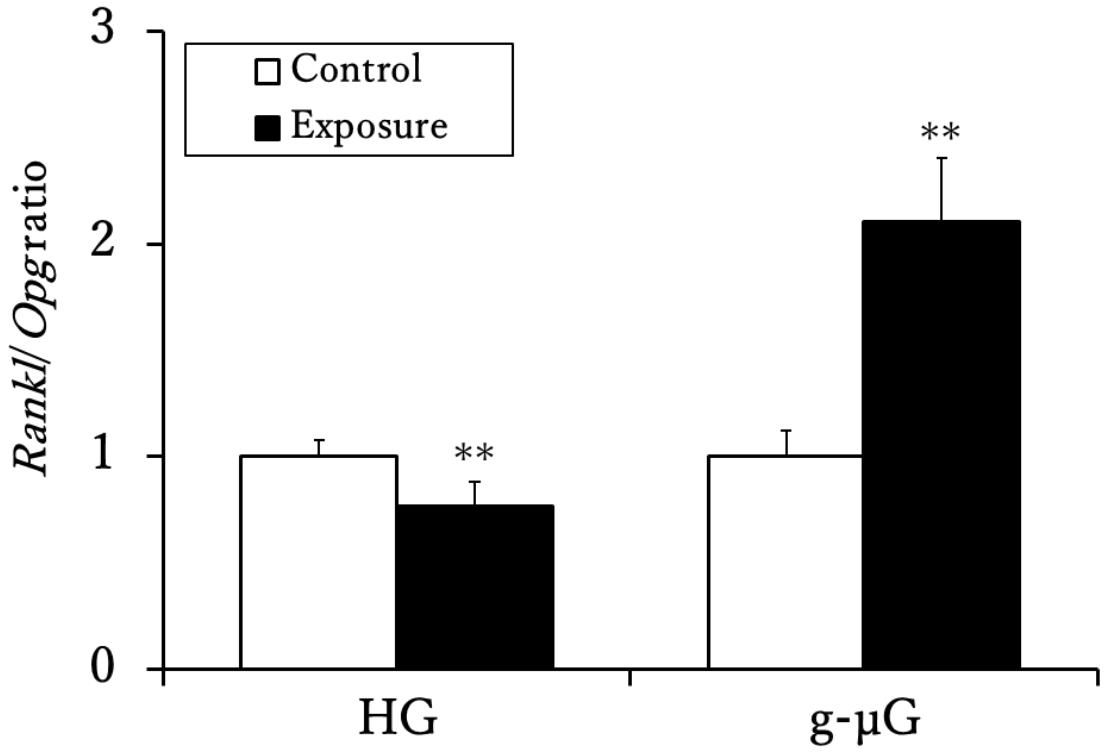

Fig. 18. The *Rankl/ Opg* ratios under hypergravity (HG) and simulated ground microgravity (g-μG). The value for the control sample was set as 1 for each gene. Data represent the mean ± S.E.M. ($n = 10$). ** $p < 0.01$ (Paired t-test).

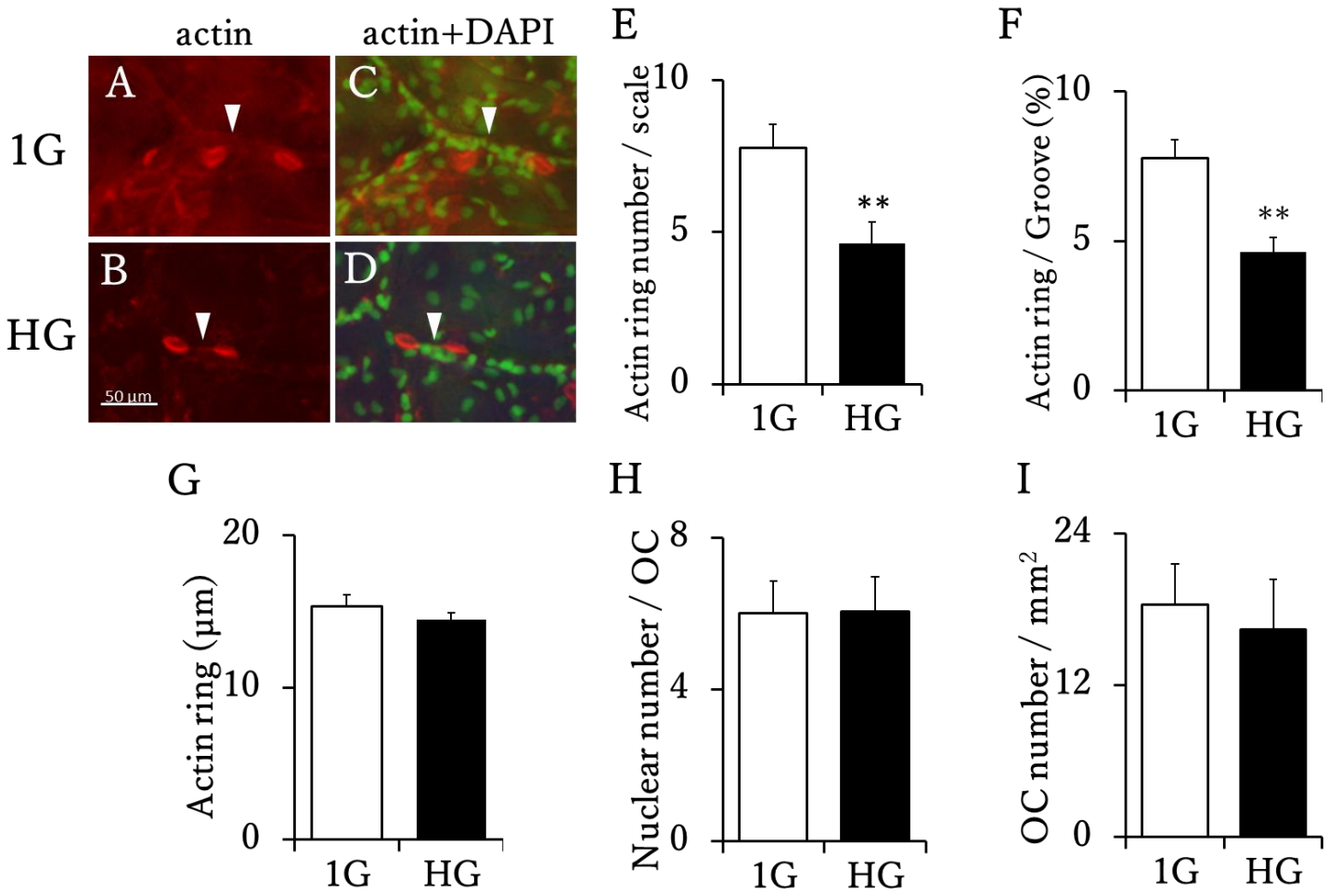

Fig. 19. Histomorphometric analysis of the osteoclasts treated with hypergravity (HG). Arrowheads indicate grooves in (A, B, C, D). Data represent the mean ± S.E.M. ($n = 10$). ** $p < 0.01$ (Paired t-test).

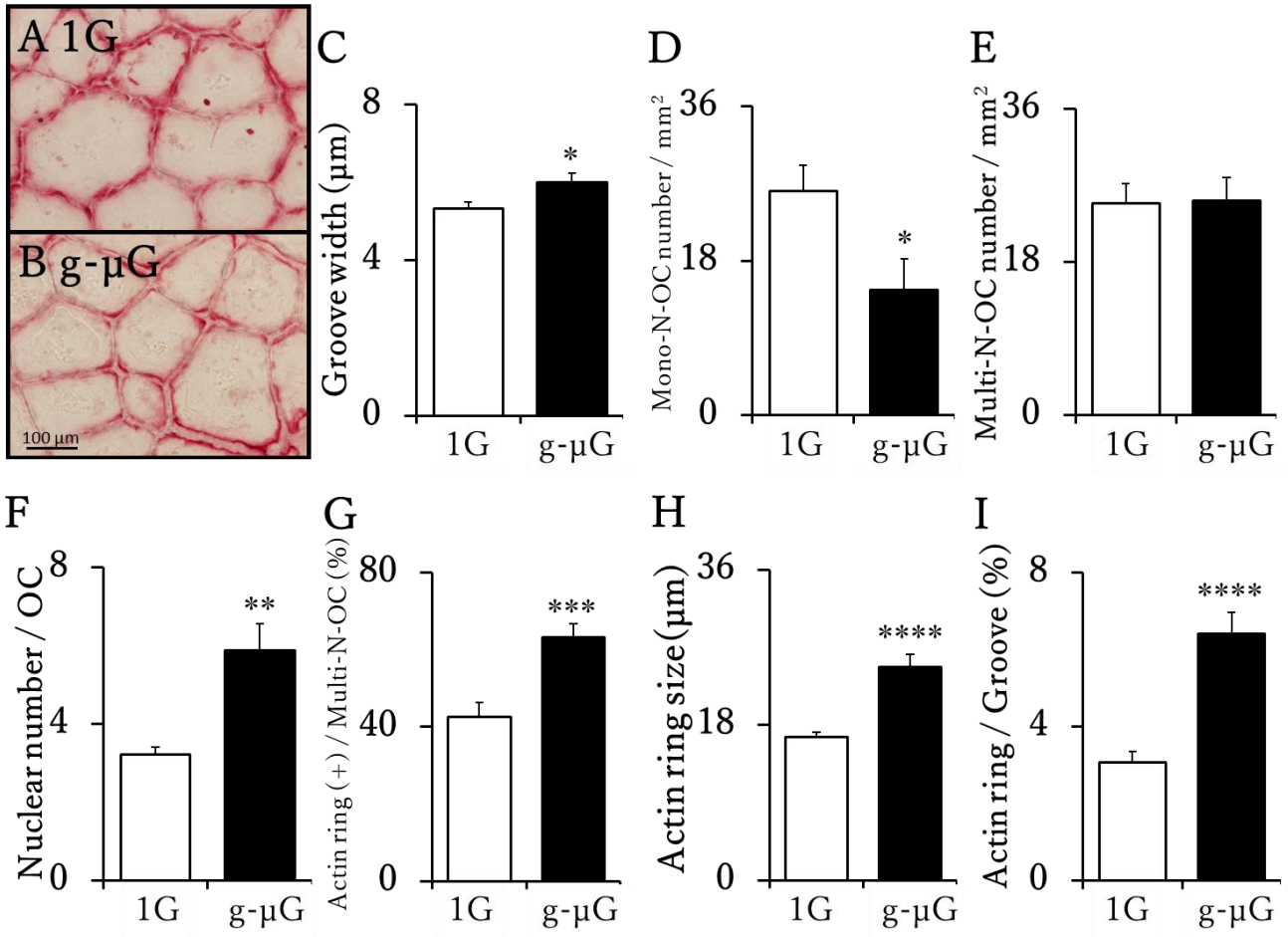

Fig. 20. Histomorphometric analysis of the osteoclasts treated with simulated ground-microgravity (g-μG). Data represent the mean ± S.E.M. ($n = 10$). * $p < 0.05$ (Paired t-test), ** $p < 0.01$ (Paired t-test), *** $p < 0.001$ (Paired t-test), and **** $p < 0.0001$ (Paired t-test).

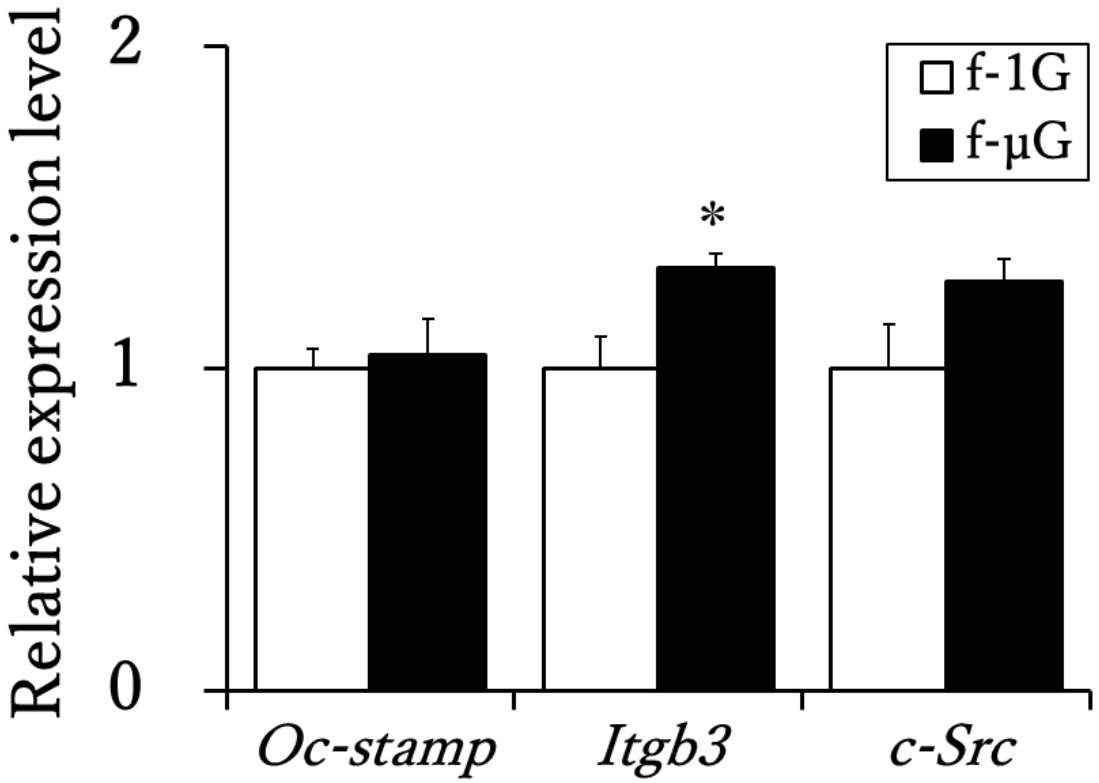

Fig. 21. Expression levels of osteoclastic marker genes under microgravity in outer space [Flight (f)-μG] and under 1 G loading in outer space [Flight(f)-1G]. The value for the control sample was set as 1 for each gene. Data represent the mean ± S.E.M. ($n = 10$). * $p < 0.05$ (Paired t-test).

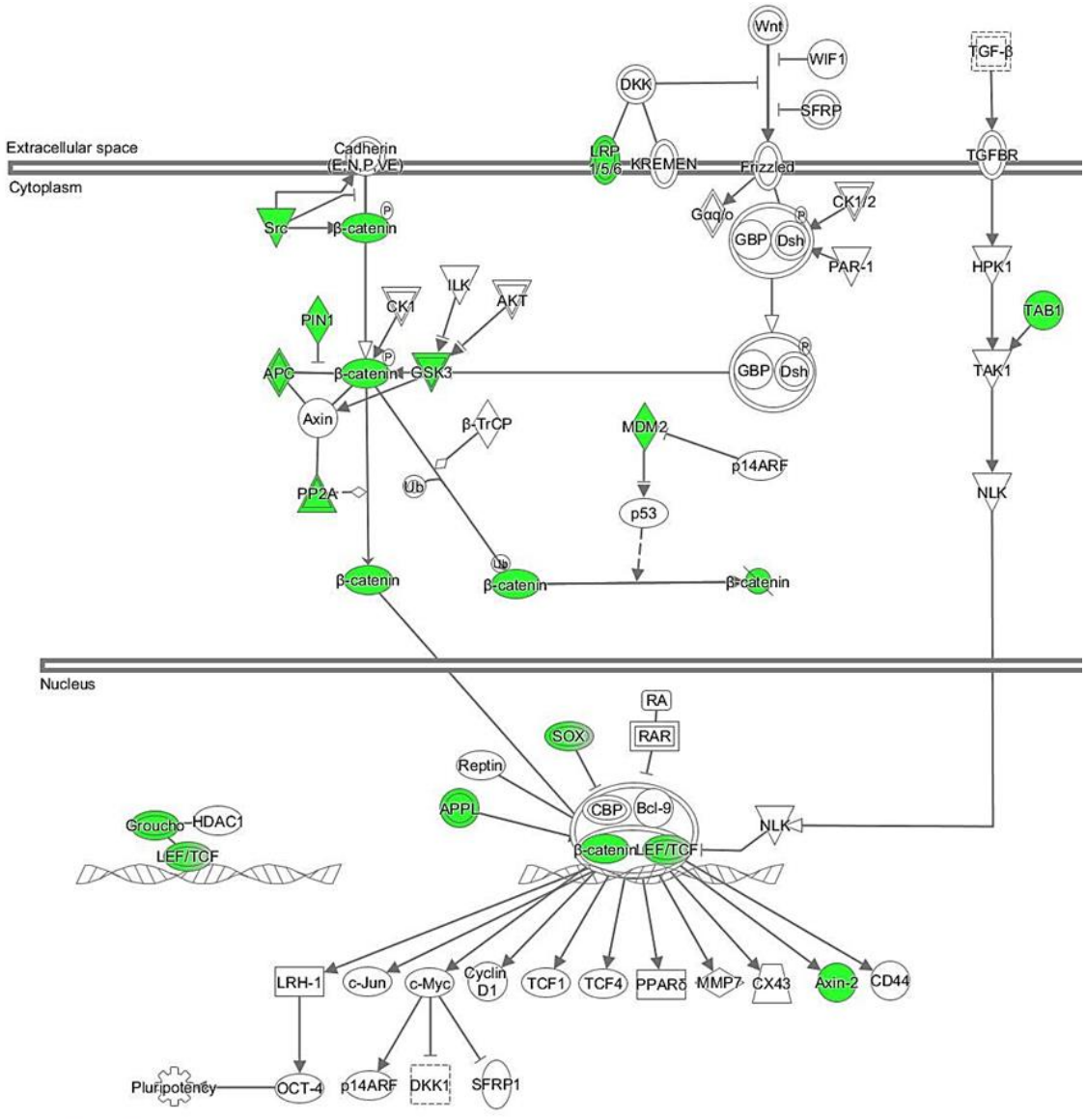

Fig. 22. Down-regulated genes linked to the canonical Wnt/ β -catenin pathway during space flight. Genes that were differentially expressed in goldfish scales during space flight were analyzed using Ingenuity® Pathway Analysis tools. Expression levels of genes in the canonical Wnt/ β -catenin pathway were down-regulated in goldfish scales cultured during space flight. Green-filled symbols indicate down-regulated genes. p-value: 8.53×10^{-4}.

Table 3. Primer sequences used for quantitative real-time PCR analysis

Target gene	Forward sequence (5' → 3')	Reverse sequence (5' → 3')
Ctsk	TGGGAGGGCTGGAAACTCAC	CATGAGCCGCATGAACCTTG
Trap	AACTTCCGCATTCCTCGAACAG	GGCCAGCCACCAGGAGATAA
Oc-stamp	TGTGGTGCTGTTTGTCCTACC	CAACCGTCCCTTCACTTCTG
Itgb3	TCCTGATGTGTTGGTGGTTG	TGCTGGTGGCTCCTTTGTAG
c-Src	AAGAAGCTCCGGCATGAGAAGC	AGGCAACCGCAGCATTTTCC
Col1a ∞	TGCAACCAGGATGCCATCAA	ATGAGGCGCAGGAAGGTGAG
Ocn	ATGCCTGAGCGCAGGTCTTC	CACAGGCCAGGTTTGCTTCA
Rankl	CGAGTGTGGCGATTTTGTTG	ATGGGCGTCTTGATTGGAAG
Opg	CGTGAACACGGTGTGCGAGTGT	CCTCTGCGCAGGCCTCACA
Dkk1	AAGCACAAGAGGAAAGGCACCCAT	TTAGTGTCTCTGGCAAGTGTGCAG
Wif1	TGCCGAAGAGCAAGGAAGC	TCCTGAAGTCGTGTGTGAATGGGG
Ef1 α	ATTGTTGCTGGTGGTGTTGG	GGCACTGACTTCCTTGGTGA

V. General Discussion

(1) Detection of RANKL-producing cells and the activation of osteoclasts by adding exogenous RANKL to goldfish scales

In the present study, RANKL-producing cells were detected in the grooves of regenerating goldfish scales. Several osteoclasts were also present. These findings suggest that RANKL-producing cells interact with osteoclasts and induce osteoclastogenesis in the grooves of regenerating scales. Therefore, I investigated the effect of exogenous RANKL on osteoclast formation in the cultured regenerating scales of goldfish. I found that recombinant mouse RANKL effectively promotes osteoclast activation in goldfish osteoclasts. The mRNA expression of the transcription factor *Nfatc1*, the master regulator of osteoclast formation, significantly increased after 3 hours of incubation with RANKL as compared to the expression level of untreated control cells. In addition, the mRNA expression of the osteoclast function gene, *Ctsk*, was significantly upregulated after 6 hours of incubation with RANKL. After incubating with RANKL for 3 and 6 hours, respectively, the mRNA expressions of *Dc-stamp* and *Oc-stamp*, which are essential for osteoclast multinucleation (Yang *et al.*, 2008; Zhang *et al.*, 2014),

were also upregulated. In addition, the mRNA expression of *Blimp1*, a factor involved in osteoclast differentiation (Miyauchi *et al.*, 2010), increased with RANKL treatment. RANKL signaling was induced by extrinsic RANKL in the osteoclasts of goldfish scales as in mammalian bone. Also, the expression of *Ephrinb2* mRNA increased significantly. After bone resorption, I estimate that EPHRIN B2 induces coupling and bone remodeling, as it does in mammalian bone (Zhao *et al.*, 2006; Matsuo and Otaki, 2012). Therefore, RANKL treatment can possibly promote the remodeling of fish scales as well as mammalian bone.

(2) SCLEROSTIN expression in the regenerating scales of goldfish and its increase due to microgravity during space flight

Whole-mount ISH and IHC were performed using regenerating goldfish scales to investigate the expression of *Sost* mRNA and SCLEROSTIN proteins in the cells of fish scales. I found that cells located along the grooves and ridges express *Sost* mRNA and its proteins on regenerating goldfish scales. Next, ISH and IHC were performed using frozen sections of regenerating scales. Signals were detected in cells covering the fibrous layer in both the central and peripheral regions of scales. Cells with ISH or IHC signals in the fiber layer were found to

have a rounded shape, suggesting that they produced a matrix of scales (Yoshikubo *et al.*, 2005; Suzuki *et al.*, 2007; Suzuki *et al.*, 2008; Ikegame *et al.*, 2019; Yamamoto *et al.*, 2020). In addition to round cells, ISH or IHC signals were detected in the flat cells lining both the bone layer along the surrounding ridge and the central mineralization matrix surface. Therefore, these results show that scale osteoblasts expressed *Sost* mRNA. In addition, a *Sost/sclerostin* signal was detected in cells half-embedded in the groove or calcification matrix. Using a transmission electron microscope, two types of semi-embedded cells were found in the bone layer. One type was observed at the bottom of the groove in contact with the collagen bundle in the fibrous layer. The other type was mostly surrounded by a mineralization matrix. Therefore, it is speculated that these half-embedded cells are osteocyte-like cells that eventually differentiate from osteoblasts and become implanted in the bone matrix, as mammalian osteocyte does (Sawa *et al.*, 2019).

Finally, outer space microgravity (F-μg) exposure increased *Sost* mRNA expression but did not affect the expression of *Dkk1* and *Wif1* mRNA. These results show for the first time that the expression of *Sost* in fish scales is stimulated by microgravity, suggesting that SCLEROSTIN is involved in the mechanisms of

bone loss in outer space.

(3) Response of osteoblasts and osteoclasts to hypergravity and microgravity using goldfish scales as a bone model

In the present study, for the first time, the responses of osteoclasts and osteoblasts to hypergravity and simulated g-μG were investigated simultaneously using goldfish scales. Results indicate that the mRNA expression of marker in osteoclasts and osteoblasts was changed to induce bone formation under 3G loading, but to induce bone resorption under simulated g-μG. These results were supported by morphological observations. The obtained findings using goldfish scales were consistent with those of mammalian *in vivo* studies (Kawao *et al.*, 2016; Chatziravdeli *et al.*, 2019; Smith, 2020).

In my study, the *Rankl*/*Opg* ratio significantly decreased with 3G loading, while the ratio increased under simulated g-μG. It was suggested that inhibitors of the *Wnt*/β-catenin signaling pathway (*Wif1* and *Dkk1*), which are important signaling pathways regulating *Opg* expression (Kubota *et al.*, 2009), are involved in this phenomenon. Both hypergravity and simulated g-μG treatments function to increase *Rankl* expression. These results indicate that the *Rankl* gene may be

generally sensitive to changes in gravity. During space flight, the expression of osteoclast marker genes increased, and several genes involved in the *Wnt/β*-catenin pathway were downregulated. These results were in agreement with the simulated g-μG results.

Under the simulated g-μG, the size of osteoclasts was enlarged, and the number of multinucleated osteoclasts increased significantly. Most of the activated osteoclasts were distributed along the edges of the scale grooves. This strongly suggests that osteoclasts activated by RANKL secreted from RANKL-producing cells are present in grooves. This is the first morphological demonstration of the response of osteoclasts to hypergravity and g-μG using the same method.

Current research results, along with the above findings using fish scales, provide evidence that an organ culture system of fish scale in which osteoclasts and osteoblasts coexist on an intact bone matrix and sensitively respond to changes in gravity, is an excellent experimental system for studying the response of bone cells to changes in gravity loading or unloading.

VI. Conclusion

Detection of RANKL-producing cells and the activation of osteoclasts by adding exogenous RANKL in goldfish scales

This study is the first to detect RANKL-producing cells in regenerating goldfish scales by preparing antiserum against goldfish RANKL in rabbits. Furthermore, I investigated the effects of exogenous RANKL on osteoclastogenesis in regenerating goldfish scales. As a result, the localization of RANKL immunopositive cells was mainly detected in the grooves of regenerating scales. In addition, treatment of regenerating scales with mammalian RANKL significantly increased the mRNA levels of both *Nfatc1* and *Ctsk*, which are molecules associated with osteoclastic multinucleation and differentiation. Therefore, I conclude that RANKL plays an important role in osteoclastogenesis in fish scales as well as mammalian bone.

SCLEROSTIN expression in regenerating scales of goldfish and its increase due to microgravity during space flight

The present study is the first to demonstrate the existence of SCLEROSTIN-

containing cells in goldfish scales. SCLEROSTIN expression in goldfish scales was shown at both mRNA and protein levels using ISH and IHC, respectively. An analysis of the shape and situation of SCLEROSTIN-expressing cells was performed in the osteoblasts of goldfish scales. In addition, osteocyte-like cells were detected in goldfish scales, which also produced SCLEROSTIN. Finally, the mRNA level of *Sost* in goldfish scales was increased by microgravity in outer space. Therefore, SCLEROSTIN is an important factor for analyzing osteoclastogenesis under microgravity.

Response of osteoblasts and osteoclasts to hypergravity and microgravity using goldfish scales as a bone model

This study for the first time investigated the responses of osteoclasts and osteoblasts to both hypergravity and simulated g-μG simultaneously using goldfish scales. An analysis of each marker mRNA expression in osteoclasts and osteoblasts showed that bone formation is enhanced by 3G loading, while bone resorption increases by simulated g-μG loading. Furthermore, morphological osteoclast activation was induced by simulated g-μG, although osteoclast deactivation was observed in 3G-treated scales. In the space experiment, the

results obtained by the g-μG simulation were reproduced. RNA-sequencing analysis revealed that osteoclastic activation was induced by the downregulation of *Wnt* signaling under flight microgravity. Therefore, I conclude that goldfish scales can be used as a bone model for analyzing the response of osteoclasts and osteoblasts to gravity.

References

Al - Bari, A. A., & Mamun, A. A., Current advances in regulation of bone homeostasis. *FASEB BioAdv.* **2**, 668-679 (2020).

Alford, A. I., Kozloff, K. M. & Hankenson, K. D., Extracellular matrix networks in bone remodeling. *Int. J. Biochem. Cell Biol.* **65**, 20-31 (2015).

Asagiri, M., Sato, K., Usami, T., Ochi, S., Nishina, H., Yoshida, H., Morita, I., Wagner, E. F., Mak, T. W., Serfling, E. & Takayanagi, H., Autoamplification of NFATc1 expression determines its essential role in bone homeostasis. *J. Exp. Med.*, **202**, 1261-1269 (2005).

Azuma, K., Kobayashi, M., Nakamura, M., Suzuki, N., Yashima, S., Iwamuro, S., Ikegame, M., Yamamoto, T. & Hattori, A., Two osteoclastic markers expressed in multinucleate osteoclasts of goldfish scales. *Biochem. Biophys. Res. Commun.* **362**, 594-600 (2007).

Balemans, W., Ebeling, M., Patel, N., Van Hul, E., Olson, P., Dioszegi, M., Kacza, C., Wuyts, W., Van Den Ende, J., Willems, P., Paes-Albes, A. F., Hill, S., Bueno, M., Ramos, F. J., Tacconi, P., Dikkers, F. G., Stratakis, C., Lindpaintner, K., Vickery, B., Foernzler, D. & Van Hul, W., Increased bone

density in sclerosteosis is due to the deficiency of a novel secreted protein (SOST). *Hum. Mol. Genet.* **10**, 537-543 (2001).

Balemans, W., Patel, N., Ebeling, M., Van Hul, E., Wuyts, W., Lacza, C., Dioszegi, M., Dikkers, F. G., Hildering, P., Willems, P. J., Verheij, J. B. G. M., Lindpaintner, K., Vickery, B., Foernzler, D. & Van Hul, W., Identification of a 52 kb deletion downstream of the SOST gene in patients with van Buchem disease. *J. Med. Genet.* **39**, 91-97 (2002).

Bereiter-Hahn, J. & Zylberberg, L., Regeneration of teleost fish scale. *Comp. Biochem. Physiol.* **105A**, 625-641 (1993).

Brockstedt, H., Bollerslev, J., Melsen, F. & Mosekilde, L., Cortical bone remodeling in autosomal dominant osteopetrosis: a study of two different phenotypes. *Bone* **18**, 67–72 (1996).

Brunkow, M. E., Gardner, J. C., Van Ness, J., Paeper, B. W., Kovacevich, B. R., Proll, S., Skonier, J. E., Zhao, L., Sabo, P. J., Fu, Y., Alisch, R. S., Gillett, L., Colbert, T., Tacconi, P., Galas, D., Hamersma, H., Beighton, P. & Mulligan, J., Bone dysplasia sclerosteosis results from loss of the SOST gene product, a novel cystine knot-containing protein. *Am. J. Hum. Genet.* **68**, 577-589 (2001).

Carmeliet, G., Vico, L. & Bouillon, R., Space flight: A challenge for normal bone homeostasis. *Crit. Rev. Eukaryot. Gene Expr.* **11**, 131-144 (2001).

Cavanagh, P. R., Licata, A. A. & Rice, A. J., Exercise and pharmacological countermeasures for bone loss during long-duration space flight. *Gravit. Space Biol. Bull.* **18**, 39-58 (2005).

Chatziravdeli, V., Katsaras, G. N. & Lambrou, G. I., Gene expression in osteoblasts and osteoclasts under microgravity conditions: A systematic review. *Curr. Genomics* **20**, 184-198 (2019).

Chen, X., Wang, Z., Duan, N., Zhu, G., Schwarz, E. M. & Xie, C., Osteoblast–osteoclast interactions. *Connect. Tissue Res.* **59**, 99-107 (2018).

Civitelli, R., Cell–cell communication in the osteoblast/osteocyte lineage. *Arch. Biochem. Biophys.* **473**, 188-192 (2008).

Cole, A. A. & Walters, L. M., Tartrate-resistant acid phosphatase in bone and cartilage following decalcification and cold-embedding in plastic. *J. Histochem. Cytochem.* **35**, 203-206 (1987).

Collette, N. M., Yee, C. S., Murugesh, D., Sebastian, A., Taher, L., Gale, N. W., Economides, A. N., Harland, R. M. & Loots, G. G., Sost and its paralog Sostdc1 coordinate digit number in a Gli3-dependent manner. *Dev. Biol.* **383**,

90-105 (2013).

Dalbeth, N. Pool, B., Smith, T., Callon, K. E., Lobo, M., Taylor, W. J., Jones, O. B., Cornish, J. & McQueen, F. M., Circulating mediators of bone remodeling in psoriatic arthritis: implications for disordered osteoclastogenesis and bone erosion. *Arthritis Res. Ther.* **12**, R164 (2010).

Delgado-Calle, J., Sato, A. Y. & Bellido, T., Role and mechanism of action of sclerostin in bone. *Bone* **96**, 29-37 (2017).

de Vrieze, E., Moren, M., Metz, J. R., Flik, G. & Lie, K. K., Arachidonic acid enhances turnover of the dermal skeleton: studies on zebrafish scales. *PLoS One* **9**, e89347 (2014).

Eimori, K., Endo, N., Uchiyama, S., Takahashi, Y., Kawashima, H. & Watanabe, K. Disrupted bone metabolism in long-term bedridden patients. *PLoS One* **11**, e0156991 (2016).

Ellies, D. L., Viviano, B., McCarthy, J., Rey, J. P., Itasaki, N., Saunders, S. & Krumlauf, R., Bone density ligand, sclerostin, directly interacts with LRP5 but not LRP5^{G171V} to modulate Wnt activity. *J. Bone Miner. Res.* **21**, 1738–1749 (2006).

Figurek, A., Rroji, M. & Spasovski, G., Sclerostin: a new biomarker of CKD-MBD.

Int. Urol. Nephrol. **52**, 107-113 (2020).

Gebken, J., Lüders, B., Notbohm, H., Klein, H. H., Brinckmann, J., Müller, P. K. & Bätge, B., Hypergravity stimulates collagen synthesis in human osteoblast-like cells: Evidence for the involvement of p44/42 MAP-kinases (ERK 1/2). *J. Biochem.* **126**, 676-682 (1999).

Gerbaix, M., Gnyubkin, V., Farlay, D., Olivier, C., Ammann, P., Courbon, G., Laroche, N., Genthial, R., Follet, H., Peyrin, F., Shenkman, B., Gauquelin-Koch, G. & Vico, L., One-month spaceflight compromises the bone microstructure, tissue-level mechanical properties, osteocyte survival and lacunae volume in mature mice skeletons. *Sci. Rep.*, **7**, 2659 (2017).

Hanmoto, T., Tabuchi, Y., Ikegame, M., Kondo, T., Kitamura, K., Endo, M., Kobayashi, I., Mishima, H., Sekiguchi, T., Urata, M., Seki, A., Yano, S., Hattori, A. & Suzuki, N., Effects of low-intensity pulsed ultrasound on osteoclasts: Analysis with goldfish scales as a model of bone. *Biomed. Res.* **38**, 71-77 (2017).

Harter, L. V., Hruska, K. A. & Duncan, R. L., Human osteoblast-like cells respond to mechanical strain with increased bone matrix protein production independent of hormonal regulation. *Endocrinology* **136**, 528-535 (1995).

Henry, J. P. & Bordoni, B., Histology, Osteoblasts. *StatPearls*. Treasure Island (FL): StatPearls Publishing (2020).

Hinton, P. V., Rackard, S. M. & Kennedy, O. D., *In vivo* osteocyte mechanotransduction: recent developments and future directions. *Curr. Osteoporos. Rep.* **16**, 746-753 (2018).

Hoffler, C. E., Hankenson, K. D., Miller, J. D., Bilkhu, S. K. & Goldstein, S. A., Novel explant model to study mechanotransduction and cell-cell communication. *J. Orthop. Res.* **24**, 1687-1698 (2006).

Ikegame, M., Hattori, A., Tabata, M.J., Kitamura, K., Tabuchi, Y., Furusawa, Y., Maruyama, Y., Yamamoto, T., Sekiguchi, T., Matsuoka, R., Hanmoto, T., Ikari, T., Endo, M., Omori, K., Nakano, M., Yashima, S., Ejiri, S., Taya, T., Nakashima, H., Shimizu, N., Nakamura, M., Kondo, T., Hayakawa, K., Takasaki, I., Kaminishi, A., Akatsuka, R., Sasayama, Y., Nishiguchi, T., Nara, M., Iseki, H., Chowdhury, V.S., Wada, S., Ijiri, K., Takeuchi, T., Suzuki, T., Ando, H., Matsuda, K., Somei, M., Mishima, H., Mikuni-Takagaki, Y., Funahashi, H., Takahashi, A., Watanabe, Y., Maeda, M., Uchida, H., Hayashi, A., Kambegawa, A., Seki, A., Yano, S., Shimazu, T., Suzuki, H. Hirayama, J. & Suzuki, N., Melatonin is a potential drug for the prevention of bone loss

during space flight. *J. Pineal Res.*, **67**, e12594 (2019).

Ishizu, H., Sekiguchi, T., Ikari, T., Kitamura, K. I., Kitani, Y., Endo, M., Urata, M., Kinoshita, Y., Hattori, A., Srivastav, A. K., Mishima, H., Mizusawa, K., Takahashi, A. & Suzuki, N., alpha-Melanocyte-stimulating hormone promotes bone resorption resulting from increased osteoblastic and osteoclastic activities in goldfish. *Gen. Comp. Endocrinol.* **262**, 99-105 (2018).

Kakikawa, M., Yamamoto, T., Chowdhury, V. S., Satoh, Y., Kitamura, K., Sekiguchi, T., Funahashi, H., Omori, K., Endo, M., Yano, S., Yamada, S., Hayakawa, K., Chiba, A., Srivastav, A. K., Ijiri, K., Seki, A., Hattori, A. & Suzuki, N., Determination of calcium sensing receptor in the scales of goldfish and induction of its mRNA expression by acceleration loading. *Biol. Sci. Space* **26**, 26-31 (2012).

Kawao, N., Morita, H., Obata, K., Tamura, Y., Okumoto, K. & Kaji, H., The vestibular system is critical for the changes in muscle and bone induced by hypergravity in mice. *Physiol. Rep.* **4**, e12979 (2016).

Kearns, A. E., Khosla, S. & Kostenuik, P. J., Receptor activator of nuclear factor kappaB ligand and osteoprotegerin regulation of bone remodeling in health

and disease. *Endocr. Rev.* **29**, 155-192 (2008).

Kitamura, K., Suzuki, N., Sato, Y., Nemoto, T., Ikegame, M., Shimizu, N., Kondo, T., Furusawa, Y., Wada, S. & Hattori, A., Osteoblast activity in the goldfish scale responds sensitively to mechanical stress. *Comp. Biochem. Physiol. Part A* **156**, 357-363 (2010).

Kobayashi, Y., Uehara, S., Udagawa, N. & Takahashi, N., Regulation of bone metabolism by Wnt signals. *J. Biochem.* **159**, 387-392 (2016).

Kondo, Y., Irie, K., Ikegame, M., Ejiri, S., Hanada, K. and Ozawa, H., Role of stromal cells in osteoclast differentiation in bone marrow. *J. Bone Miner. Metab.* **19**, 352-358 (2001).

Kubota, T., Michigami, T. & Ozono, K., Wnt Signaling in bone metabolism. *J. Bone Miner. Metab.* **27**, 265-271 (2009).

Lacey, D. L., Boyle, W. J., Simonet, W. S., Kostenuik, P. J., Dougall, W. C., Sullivan, J. K., Martin, J. S. & Dansey, R., Bench to bedside: Elucidation of the OPG-RANK-RANKL pathway and the development of denosumab. *Nat. Rev. Drug Discov.* **11**, 401-419 (2012).

Lerner, U. H., Bone remodeling in post-menopausal osteoporosis. *J. Dent. Res.* **85**, 584–595 (2006).

Lin, C., Jiang, X., Dai, Z., Guo, X., Weng, T., Wang, J., Li, Y., Feng, G., Gao, X. & He, L., Sclerostin mediates bone response to mechanical unloading through antagonizing Wnt/β-catenin signaling. *J. Bone Miner. Res.* **24**, 1651-1661 (2009).

Li, X., Zhang, Y., Kang, H., Liu, W., Liu, P., Zhang, J., Harris, S. E. & Wu, D., Sclerostin binds to LRP5/6 and antagonizes canonical Wnt signaling. *J. Biol. Chem.* **280**, 19883-19887 (2005).

Macaulay, T. R., Siamwala, J. H., Hargens, A. R. & Macias, B. R., Thirty days of spaceflight does not alter murine calvariae structure despite increased *Sost* expression. *Bone Rep.* **7**, 57-62 (2017).

Makihira, S., Kawahara, Y., Yuge, L., Mine, Y. & Nikawa, H., Impact of the microgravity environment in a 3-dimensional clinostat on osteoblast- and osteoclast-like cells. *Cell Biol. Int.* **32**, 1176-1181 (2008).

Matsuo, K. & Otaki, N., Bone cell interactions through Eph/ephrin bone modeling, remodeling and associated diseases. *Cell Adh. Migr.* **6**, 148-156 (2012).

Miyauchi, Y., Ninomiya, K., Miyamoto, H., Sakamoto, A., Iwasaki, R., Hoshi, H., Miyamoto, K., Hao, W., Yoshida, S., Morioka, H., Chiba, K., Kato, S., Tokuhisa, T., Saitou, M., Toyama, Y., Suda, T. & Miyamoto, T., The Blimp1-

Bcl6 axis is critical to regulate osteoclast differentiation and bone homeostasis. *J. Exp. Med.* **207**, 751-762 (2010).

Nagy, V. & Penninger, J. M., The RANKL-RANK story. *Gerontology* **61**, 534-542 (2015).

Nakashima, T., Hayashi, M., Fukunaga, T., Kurata, K., Oh-Hora, M., Feng, J. Q., Bonewald, L. F., Kodama, T., Wutz, A., Wagner, E. F., Penninger, J. F. & Takayanagi, H., Evidence for osteocyte regulation of bone homeostasis through RANKL expression. *Nat. Med.* **17**, 1231-1234 (2011).

Nemoto, A. & Uemura, T., Hypergravity effects on osteoclasts activity. *J. Gravit. Physiol.* **7**, P127-128 (2000).

Nishimoto, S. K., Araki, N., Robinson, F. D. & Waite, J. H., Discovery of bone gamma-carboxyglutamic acid protein in mineralized scales. *J. Biol. Chem.* **267**, 11600-11605 (1992).

Ohira, Y., Shimizu, M., Ura, K. & Takagi, Y., Scale regeneration and calcification in goldfish *Carassius auratus*: Quantitative and morphological processes. *Fisherys Sci.* **73**, 46-54 (2007).

Omori, K., Wada, S., Maruyama, Y., Hattori, A., Kitamura, K., Sato, Y., Nara, M., Funahashi, H., Yachiguchi, K., Hayakawa, K., Endo, M., Kusakari, R., Yano,

S., Srivastav, A.K., Kusui, T., Ejiri, S., Chen, W., Tabuchi, Y., Furusawa, Y., Kondo, T., Sasayama, Y. Nishiuchi, T., Nakano, M., Sakamoto, T. & Suzuki, N., Prostaglandin E_2 increases both osteoblastic and osteoclastic activities in the scales and participates in calcium metabolism in goldfish. *Zool. Sci.* **29**, 499-504 (2012).

Ono, T. & Nakashima, T., Recent advances in osteoclast biology. *Histochem. Cell Biol.* **149**, 325-341 (2018).

Onozato, H. & Watabe, N., Studies on fish scale formation and resorption III: Fine structure and calcification of the fibrillary plates of the scales in *Carassius auratus* (Cypriniformes: Cyprinidae). *Cell Tissue Res.* **201**, 409-422 (1979).

Owan, I., Burr, D. B., Turner, C. H., Qiu, J., Tu, Y., Onyia, J. E. & Duncan, R. L., Mechanotransduction in bone: Osteoblasts are more responsive to fluid forces than mechanical strain. *Am. J. Physiol.* **273**, C810-C815 (1997).

Pajevic, P. D., Spatz, J. M., Garr, J., Adamson, C. & Misener, L., Osteocyte biology and space flight. *Curr. Biotechnol.* **2**, 179-183 (2013).

Poole, K. E., van Bezooijen, R. L., Loveridge, N., Hamersma, H., Papapoulos, S. E., Löwik, C. W. & Reeve, J., Sclerostin is a delayed secreted product of osteocytes that inhibits bone formation. *FASEB J.* **19**,1842-1844 (2005).

Robling, A. G., Niziolek, P. J., Baldridge, L. A., Condon, K. W., Allen, M. R., Alam, Im., Mantila, S. M., Gluhak-Heinrich, J., Bellido, T. M., Harris, S. E. & Turner, C. H., Mechanical stimulation of bone *in vivo* reduces osteocyte expression of Sost/sclerostin. *J. Biol. Chem.* **283**, 5866-5875 (2008).

Rucci, N., Rufo, A., Alamanou, M. & Teti, A., Modeled microgravity stimulates osteoclastogenesis and bone resorption by increasing osteoblast RANKL/OPG ratio. *J. Cell Biochem.* **100**, 464-473 (2007).

Sambandam, Y., Blanchard, J. J., Daughtridge, G., Kolb, R. J., Shanmugarajan, S., Pandruvada, S. N. M., Bateman, T. A. & Reddy, S. V., Microarray profile of gene expression during osteoclast differentiation in modelled microgravity. *J. Cell Biochem.* **111**, 1179–1187 (2010).

Saito, M., Soshi, S. & Fujii, K., Effect of hyper- and microgravity on collagen post-translational controls of MC3T3-E1 osteoblasts. *J. Bone Miner. Res.* **18**, 1695-1705 (2003).

Sato, M., Yachiguchi, K., Motohashi, K., Yaguchi, Y., Tabuchi, Y., Kitani, Y., Ikaria, T., Ogiso, S., Sekiguchi, T., Hai, T. N., Huong, D. T. T., Hoang, N. V., Urata, M., Mishima, H., Hattori, A. & Suzuki, N., Sodium fluoride influences calcium metabolism resulting from the suppression of osteoclasts

in the scales of nibbler fish *Girella punctate*. *Fisheries Sci.* **83**, 543-550 (2017).

Sawa, N., Fujimoto, H., Sawa, Y. & Yamashita, J., Alternating differentiation and dedifferentiation between mature osteoblasts and osteocytes. *Sci. Rep.* **9**, 13842 (2019).

Saxena, R., Pan, G., Dohm, E. D. & McDonald, J. M., Modeled microgravity and hindlimb unloading sensitize osteoclast precursors to RANKL-mediated osteoclastogenesis. *J. Bone Miner. Metab.* **29**, 111–122 (2011).

Schaffler, M. B. & Kennedy, O. D., Osteocyte signaling in bone. *Curr. Osteoporos. Rep.* **10**, 118-125 (2012).

Schaffler, M. B., Cheung, W. Y., Majeska, R., & Kennedy, O., Osteocytes: master orchestrators of bone. *Calcif. Tissue Int.* **94**, 5-24 (2014).

Schneider, V., Oganov, V., LeBlanc, A., Rakmonov, A., Taggart, L., Bakulin, A., Huntoon, C., Grigoriev, A. & Varonin, L., Bone and body mass changes during space flight. *Acta Astronaut.* **36**, 463-466 (1995).

Searby, N. D., Steele, C. R. & Globus, R. K., Influence of increased mechanical loading by hypergravity on the microtubule cytoskeleton and prostaglandin E_2 release in primary osteoblasts. *Am. J. Physiol.* **289**, C148-C158 (2005).

Silva, I. & Branco, J. C., RANK/RANKL/OPG: Literature review. *Acta Reumatol.*

Port. **36**, 209-218 (2011).

Smith, J. K., Osteoclasts and microgravity. *Life* **10**, 207 (2020).

Staehling-Hampton, K., Proll, S., Paeper, B. W., Zhao, L., Charmley, P., Brown, A., Gardner, J. C., Galas, D., Schatzman, R. C., Beighton, P., Papapoulos, S., Hamersma, H. & Brunkow, M. E., A 52-kb deletion in the SOST-MEOX1 intergenic region on 17q12-q21 is associated with van Buchem disease in the Dutch population. *Am. J. Med. Genet.* **110**, 144-152 (2002).

Suzuki, N., Danks, J. A., Maruyama, Y., Ikegame, M., Sasayama, Y., Hattori, A., Nakamura, M., Tabata. M. J., Yamamoto, T., Furuya, R., Saijoh, K., Mishima, H., Srivastav, A. K., Furusawa, Y., Kondo, T., Tabuchi, Y., Takasaki, I., Chowdhury, V. S., Hayakawa, K. & Martin, T. J., Parathyroid hormone 1 (1-34) acts on the scales and involves calcium metabolism in goldfish. *Bone* **48**, 1186-1193 (2011).

Suzuki, N., Hanmoto, T., Yano, S., Furusawa, Y., Ikegame, M., Tabuchi, Y., Kondo, T., Kitamura, K., Endo, M., Yamamoto, T., Sekiguchi, T., Urata, M., Mikuni-Takagaki, Y. & Hattori, A., Low-intensity pulsed ultrasound induces apoptosis in osteoclasts: Fish scales are a suitable model for analysis of bone metabolism by ultrasound. *Comp. Biochem. Physiol. Part A* **195**, 26-31

(2016).

Suzuki, N. & Hattori, A., Melatonin suppresses osteoclastic and osteoblastic activities in the scales of goldfish. *J. Pineal Res.* **33**, 253-258 (2002).

Suzuki, N., Kitamura, K. & Hattori, A., Fish scale is a suitable model for analyzing determinants of skeletal fragility in type 2 diabetes. *Endocrine* **54**, 575–577 (2016).

Suzuki, N., Kitamura, K., Nemoto, T., Shimizu, N., Wada, S., Kondo, T., Tabata, M.J., Sodeyama, F., Ijiri, K. & Hattori, A., Effect of vibration on osteoblastic and osteoclastic activities: Analysis of bone metabolism using goldfish scale as a model for bone. *Adv. Space Res.* **40**, 1711-1721 (2007).

Suzuki, N., Kitamura, K., Omori, K., Nemoto, T., Satoh, Y., Tabata, M. J., Ikegame, M., Yamamoto, T., Ijiri, K., Furusawa, Y., Kondo, T., Takasaki, I., Tabuchi, Y., Wada, S., Shimizu, N., Sasayama, Y., Endo, M., Takeuchi, T., Nara, M., Somei, M., Maruyama, Y., Hayakawa, K., Shimazu, T., Shigeto, Y., Yano, S. & Hattori, A., Response of osteoblasts and osteoclasts in regenerating scales to gravity loading. *Biol. Sci. Space* **23**, 211-217 (2009).

Suzuki, N., Omori, K., Nakamura, M., Tabata, M.J., Ikegame, M., Ijiri, K., Kitamura, K., Nemoto, T., Shimizu, N., Kondo, T., Matsuda, K., Ando, H.,

Kasahara, H., Nagase, M., Nara, M. & Hattori, A. Scale osteoblasts and osteoclasts sensitively respond to low-gravity loading by centrifuge. *Biol. Sci. Space* **22**, 3-7 (2008b).

Suzuki, N., Somei, M., Seki, A., Reiter, R. J. & Hattori, A., Novel bromomelatonin derivatives as potentially effective drugs to treat bone diseases. *J. Pineal Res.* **45**, 229-234 (2008a).

Suzuki, N., Suzuki, T. & Kurokawa, T., Suppression of osteoclastic activities by calcitonin in the scales of goldfish (freshwater teleost) and nibbler fish (seawater teleost). *Peptides* **21**, 115-124 (2000).

Tabuchi, Y., Takasaki, I., Doi, T., Ishii, Y., Sakai, H. & Kondo, T., Genetic networks responsive to sodium butyrate in colonic epithelial cells. *FEBS Lett.* **580**, 3035-3041 (2006).

Takayanagi, H., Kim, S., Koga, T., Nishina, H., Isshiki, M., Yoshida, H., Saiura, A., Isobe, M., Yokochi, T., Inoue, J., Wagner, E.F., Mak, T.W., Kodama, T. & Taniguchi, T., Induction and activation of the transcription factor NFATc1 (NFAT2) integrate RANKL signaling in terminal differentiation of osteoclasts. *Dev. Cell* **3**, 889–901 (2002).

Tamma, R., Colaianni, G., Camerino, C., Di Benedetto, A., Greco, G., Strippoli,

M., Vergari, R., Grano, A., Mancini, L., Mori, G., Colucci, S., Grano, M. & Zallone, A., Microgravity during spaceflight directly affects *in vitro* osteoclastogenesis and bone resorption. *FASEB J.* **23**, 2549-2554 (2009).

Tatsumi, S., Ishii, K., Amizuka, N., Li, M., Kobayashi, T., Kohno, K., Ito, M., Takeshita, S. & Ikeda, K., Targeted ablation of osteocytes induces osteoporosis with defective mechanotransduction. *Cell Metab.* **5**, 464-475 (2007).

Teitelbaum, S. L., Bone resorption by osteoclasts. *Science*, **289,** 1504-1508 (2000).

Thamamongood, T. A., Furuya, R., Fukuba, S., Nakamura, M., Suzuki, N. & Hattori, A. Expression of osteoblastic and osteoclastic genes during spontaneous regeneration and autotransplantation of goldfish scale: A new tool to study intramembranous bone regeneration. *Bone* **50**, 1240-1249 (2012).

Thiel, C. S., Hauschild, S., Huge, A., Tauber, S., Lauber, B. A., Polzer, J., Paulsen, K., Lier, H., Engelmann, F., Schmitz, B., Schütte, A., Layer, L. E. & Ullrich, O., Dynamic gene expression response to altered gravity in human T cells. *Sci. Rep.* **7**, 5204 (2017).

Vico, L., Bourrin, S., Genty, C., Palle, S. & Alexandre, C., Histomorphometric

analyses of cancellous bone from COSMOS 2044 rats. *J. Appl. Physiol.* **75**, 2203–2208 (1993).

Watabe, H., Furuhama, T., Tani-Ishii, N. & Mikuni-Takagaki, Y., Mechanotransduction activates $\alpha_5\beta_1$ integrin and PI3K/Akt signaling pathways in mandibular osteoblasts. *Exp. Cell Res.* **317**, 2642-2649 (2011).

Wijenayaka, A. R., Kogawa, M., Lim, H. P., Bonewald, L. F., Findlay, D. M. & Atkins, G. J., Sclerostin stimulates osteocyte support of osteoclast activity by a RANKL-dependent pathway. *PLoS One* **6**, e25900 (2011).

Wronski, T. J. & Morey, E. R., Skeletal abnormalities in rats induced by simulated weightlessness. Metab. *Bone Dis. Relat. Res.* **4**, 69–75 (1982).

Yachiguchi, K., Sekiguchi, T., Nakano, M., Hattori, A., Yamamoto, M., Kitamura, K., Maeda, M., Tabuchi, Y., Kondo, T., Kamauchi, H., Nakabayashi, H., Srivastav, A. K., Hayakawa, K., Sakamoto, T. & Suzuki, N., Effect of inorganic mercury and methylmercury on osteoclasts and osteoblasts in the scales of the marine teleost as a model system of bone. *Zool. Sci.* **31**, 330-337 (2014).

Yamamoto, T., Ikegame, M., Hirayama, J., Kitamura, K., Tabuchi, Y., Furusawa, Y., Sekiguchi, T., Endo, M., Mishima, H., Seki, A., Yano, S., Matsubara, H., Hattori, A. & Suzuki, N., Expression of sclerostin in the regenerating scales

of goldfish and its increase under microgravity during space flight. *Biomed. Res. (Tokyo)* **41**, 279-288 (2020b).

Yamamoto, T., Ikegame, M., Kawago, U., Tabuchi, Y., Hirayama, J., Sekiguchi, T., Furusawa, Y., Yachiguchi, K., Matsubara, H., Urata, M., Hattori, A. & Suzuki, N., Detection of RANKL-producing cells and osteoclastic activation by the addition of exogenous RANKL in the regenerating scales of goldfish. *Biol. Sci. Space* **34**, 34-40 (2020a).

Yamashita, T., Yao, Z., Li, F., Zhang, Q., Badell, I. R., Schwarz, E. M., Takeshita, S., Wagner, E. F., Noda, M., Matsuo, K., Xing, L. & Boyce, B. F., NF- κ B p50 and p52 regulate receptor activator of NF- κ B ligand (RANKL) and tumor necrosis factor-induced osteoclast precursor differentiation by activating c-Fos and NFATc1. *J. Biol. Chem.* **282**, 18245-18253 (2007).

Yang, M., Birnbaum, M.J., MacKay, C.A., Mason-Savas, A., Thompson, B. & Odgren, P.R., Osteoclast stimulatory transmembrane protein (OC - STAMP), a novel protein induced by RANKL that promotes osteoclast differentiation. *J. Cell. Physiol.* **215**, 497-505 (2008).

Yano, S., Preparation and overview of fish scales experiment. *Space Utiliz. Res.* **27**, 213-216 (2011).

Yano, S., Kitamura, K., Satoh, Y., Nakano, M., Hattori, A., Sekiguchi, T., Ikegame, M., Nakashima, H., Omori, K., Hayakawa, K., Chiba, A., Sasayama, Y., Ejiri, S., Mikuni-Takagaki, Y., Mishima, H., Funahashi, H., Sakamoto, T. & Suzuki, N., Static and dynamic hypergravity responses of osteoblasts and osteoclasts in medaka scales. *Zool. Sci.* **30**, 217-223 (2013).

Yano, S., Masuda, D., Kasahara, H., Omori, K., Higashibata, A., Asashima, M., Ohnishi, T., Yatagai, F., Kamisaka, S., Furusawa, T., Higasitani, A., Majima, H., Nikawa, T., Wakabayashi, K., Takahashi, H., Suzuki, H., Shimazu, T., Hattori, A., Tanigaki, F., Shirakawa, M., Takaoki, M., Nakamura, T., Yoshimura, Y., Suzuki, N. & Ishioka, N., Excellent thermal control ability of cell biology experiment facility (CBEF) for ground-basis experiments and experiments onboard the Kibo Japanese experiment module of international space station. *Biol. Sci. Space* **26**, 12-20 (2012).

Yoshikubo, H., Suzuki, N., Takemura, K., Hoso, M., Yashima, S., Iwamuro, S., Takagi, Y., Tabata, M. J. & Hattori, A., Osteoblastic activity and estrogenic response in the regenerating scale of goldfish, a good model of osteogenesis. *Life Sci.* **76**, 2699-2709 (2005).

Zhao, C., Irie, N., Takada, Y., Shimoda, K., Miyamoto, T., Nishiwaki, T., Suda, T.

and Matsuo, K., Bidirectional ephrinB2-EphB4 signaling controls bone homeostasis. *Cell Metab.* **4**, 111-121 (2006).

Zhang, C., Dou, C.E., Xu, J. & Dong, S., DC-STAMP, the key fusion-mediating molecule in osteoclastogenesis. *J. Cell. Physiol.* **229**, 1330-1335 (2014).

Zhou, S., Zu, Y., Sun, Z., Zhuang, F. & Yang, C., Effects of hypergravity on osteopontin expression in osteoblasts. *PLoS One* **10**, e0128846 (2015).

Zylberberg, L., Bonaventure, J., Cohen-Solal, L., Hartmann, D. J. & Bereiter-Hahn, J., Organization and characterization of fibrillar collagens in fish scales in situ and in vitro. *J. Cell Sci.* **103**, 273-285 (1992).

Acknowledgements

I am deeply grateful for the guidance of many people in compiling this research.

In advancing this research, Professor Nobuo Suzuki gave me a lot of advice and guidance as an instructor and the chief examiner of this paper. I would like to thank you from the bottom of my heart. I would also like to express our sincere gratitude to Professor Hajime Matsubara, Associate Professor Isao Kobayashi, Associate Professor Azuma Taoka, and Associate Professor Toshio Sekiguchi for undertaking the assistant professor of this research. I would like to express my gratitude once again for providing appropriate advice and a useful forum for discussion after scrutinizing the paper.

This research was able to obtain results with the great cooperation of the following many people. Professor Atsuhiko Hattori of Tokyo Medical and Dental University, Professor Yoshiaki Tabuchi of University of Toyama, Professor Jun Hirayama of Komatsu University, Professor Keiichiro Kitamura of Kanazawa University, Associate Professor Mika Ikegame of Okayama University, Associate Professor Yukihiro Furusawa of Toyama Prefectural University, Associate Professor Masato Endo of Tokyo University of Marine Science and Technology, Dr. Azusa Seki of Hamley Co., Ltd., Dr. Sachiko Yano of Japan Aerospace Exploration Agency. I would like to express my deepest gratitude here.

I would also like to express my sincere gratitude to Dr. Katsuhisa Yamada, Director of Deep Sea Water Laboratories, DHC Co., Ltd., and Dr. Masaki Ishigai, President of Pharmaron Japan LLC, for their great cooperation in advancing to the doctoral program at Kanazawa University Graduate School.

Finally, I would like to express my appreciation to my parents, my beloved wife Hana and my sons Masahito, Takahito, Akihito and Tomohito for supporting my life.

Abbreviation

BLIMP1: B-lymphocyte-induced maturation protein 1

BSA: bovine serum albumin

CBEF: Cell Biology Experimental Facility

COL1A: collagen type I alpha 1

CTSK: cathepsin K

C-SRC: cellular-Src

DAPI: 4',6-diamidino-2-phenylindole

DC-STAMP: dendritic cell-specific transmembrane protein

DDBJ: DNA Data Bank of Japan

DIG: digoxigenin

DKK1: Dickkopf-related protein 1

EF1 α : elongation factor 1 α

EDTA: ethylenediaminetetraacetic acid

FCS: foetal calf serum

IHC: immunohistochemistry

ISH: *in situ* hybridization

ISS: International Space Station

LIPUS: low intensity pulsed ultrasound

MEU: measurement experiment unit

Ms-222: ethyl 3-aminobenzoate methanesulfonic acid salt

NFATc1: nuclear factor of activated T cells

OC-STAMP: osteoclast stimulatory transmembrane protein

OCN: osteocalcin

OPG: osteoprotegerin

PBS: phosphate-buffered saline

PCR: polymerase chain reaction

PFA: paraformaldehyde

PGE_2: prostaglandin E_2

PTH: parathyroid hormone

RANK: receptor activator of NF κ B

RANKL: receptor activator of NF κ B ligand

SDS: sodium lauryl sulfate

SEM: standard error of the mean

SOST: sclerostin

SSC: saline-sodium citrate

STS-132: Space Shuttle Atlantis-132

TRAP: tartrate-resistant acid phosphatase

WIF1: Wnt inhibitory factor 1